AN ANALYSIS OF THE LINK BETWEEN DEUBIQUITINATING ENZYMES AND ALS

by

Darius Farzad

A thesis submitted to Johns Hopkins University in conformity with the requirements for the degree of Master of Science.

Baltimore, Maryland

September, 2014

Abstract

Our lab has investigated a model for the pathogenesis of the neurodegenerative disease amyotrophic lateral sclerosis (ALS) that involves aggregates of a mutant form of the protein SOD1 (mSOD1-G85R). We have identified proteins of interest that may be related to the process of mSOD1 aggregate formation through assays such as worm siRNA screens and microarray analysis.

The primary focus of this thesis research is an experiment we conducted to corroborate a previous finding – namely that altering the expression of a specific deubiquitinating enzyme (DUB) has an impact on mSOD1-G85R aggregate formation – and thereby build support for a hypothesis we are developing regarding ALS pathogenesis. In addition to further investigating the relationship between this DUB and mSOD1-G85R, we conducted a microarray analysis that helped identify other proteins that may be related functionally to the DUB. In conjunction with a search of background literature, the microarray analysis uncovered several proteins of interest involved in tumor suppression pathways and copper homeostasis. A few models are proposed here for the possible link between these proteins of interest, the DUB we are investigating, and mSOD1-G85R aggregation with the goal of elucidating a pathogenetic mechanism underlying ALS.

It can be concluded from the experimental results described in this thesis that further testing must be done to verify and subsequently better understand our proposed link between the expression of the DUB we identified and mSOD1 aggregation.

Acknowledgements

Completing this project has been a long, painstaking, and ultimately rewarding process, and it would not have been possible without the support and patience of many people. I would like to thank all of the members of Dr. Wang's lab with whom I had the pleasure of working. I learned an immeasurable amount from all of you not just about laboratory science, but also about the value of a maintaining a solid work ethic each and every day. Dr. Wang set the standard for all of us in this regard and I truly appreciate the opportunity you gave me to learn and grow in this environment. I would especially like to thank Goran Periz for his support that began before I even started working in lab. You were always incredibly patient and encouraging, and I was extremely fortunate to have you guide me through this experience.

I would also like to take this opportunity to thank Dr. Evans and Dr. Hardwick. I am truly appreciative of all of your patience, feedback, and support and I know that my efforts on this project were maximized thanks to your contributions. While I feel that I got the most out of my thesis thanks to my committee members, I know that I owe a huge debt of gratitude to Sharon Warner for helping me actually complete this project. What was already a long process might have turned into a lifelong project if it was not for your assistance. I would also like to thank Shannon Gaston for your assistance in the latter stages of this process which allowed me to get to the finish line.

Finally, I would like to thank my friends and family for their constant support. Whether it was through encouraging words or derision for my ongoing struggles, you all helped me get to where I needed to go. I especially would like to thank my sister Maryam and my friend Sara Ghayouri for helping me develop a significantly more

presentable final product through their editing and specific guidance. To all of my friends, I would like to apologize for ending your favorite running joke. I would also like to thank my parents, sister, brother, and their beautiful families. I do not think someone could benefit more from having their life enriched in so many different ways by those closest to them as I have. I could never earn all that you have given and continue to give me, but I will try as hard as I can to do so.

Table of Contents

Table of Figures

Table of Tables

An Analysis of the Link between Deubiquitinating Enzymes and ALS

Introduction

Amyotrophic lateral sclerosis (ALS) has been recognized as a deadly disease since it was named Lou Gehrig's Disease after the early 20th century baseball legend. While a great deal has been discovered about ALS since it claimed his life, there are still many unknowns regarding what triggers this disease and how the known effect of motor neuron degeneration arises. Genetic studies on patients and extensive laboratory research – particularly over the past 20 years – have revealed several specific proteins and biochemical pathways that seem to have important roles in ALS pathogenesis. In spite of this progress, there are still no significantly effective therapies to treat this disease, and the proper diagnosis itself can only be made based on clinical presentation due to the lack of a specific test or biomarker [1]. Despite the advances in the field, the molecular understanding of the disease remains unsolved [1].

While there is not a clear map that depicts how ALS pathogenesis occurs, relations can be drawn between the various proteins and pathways that have been clearly identified through research as being linked to this disease. The cellular components and processes that have been implicated in ALS development include defects in transcription regulation, mitochondrial dysfunction, axonal transport, and the primary focus of this paper – the ubiquitin proteasome system (UPS) [3-5]. This topic was the driving force for much of my laboratory work because our research team had previously investigated a link between SOD1 aggregation and a component of the UPS, the enzyme USP7.

Further research is required to determine what types of cellular stress induce the destructive alterations in the aforementioned systems, and the manner in which the

defective functioning of some or all of these processes leads to motor neuron degeneration. Here I will delve into the topic of deubiquitinating enzymes, specifically USP7, and how recent research including the work done in our laboratory has shown that the manipulation of USP7 and other components of the UPS may have an impact on the disease phenotype that is displayed in ALS cases.

ALS General Background

While there is still much to be discovered about ALS pathogenesis on the molecular level, the broader physiological effects of this disease have been well-documented. Degeneration of neurons occurs in the upper motor neurons (UMN's), which link the motor cortex within the brain to the spinal cord, as well as the lower motor neurons (LMN's), which connect the central nervous system to muscle [3]. A general trend of disease progression has been noted in which the first signs appear asymmetrically in the limbs, and the spread of disease is eventually manifested as generalized limb muscle weakness [8]. Aside from the symptoms of muscle weakness and paralysis that arise given this pathology, some ALS patients also suffer from difficulties with speaking, swallowing, and breathing normally [1, 3].

ALS cases have been divided into four categories: limb-onset ALS, bulbar-onset ALS (which includes patients suffering from speech and swallowing difficulties), primary lateral sclerosis (a rarer diagnosis in the case of which only UMN's are affected), and progressive muscular atrophy (in which only LMN's are affected). This disease can also be subcategorized based on the presence of both sporadic ALS cases (sALS), which include the majority of patients, and familial cases (fALS), which comprise 5-10% of ALS patients. In addition to the prevalence rates of these two forms of ALS, a difference

in the patient demographics has also been observed, as the age range for the peak onset of disease has been reported as being earlier in the familial form of disease (47-52 years) compared to the sporadic form (58-63 years) [1].

These variations within the spectrum of ALS cases also include predictors that are associated with increased or reduced patient survival; factors such as old age and early respiratory muscle dysfunction indicate a poorer patient prognosis, while factors such as limb-onset disease indicate the likelihood of prolonged survival [1]. Other measures that are used to evaluate the prognosis for an ALS patient are rate of disease progression and nutritional status. Regardless of each ALS patient's prognostic factors, the diagnosis is usually a terminal one with most patients typically dying from the disease within a short time-span [1]. It has been reported that only 50% of ALS patients survive the first 30 months following the appearance of disease symptoms, and that this number drops to approximately 20% after five to ten years [1].

The treatment options for ALS are limited, although these methods can have some effect on the progression and burden of disease in these patients. The primary drug that has been used in these cases is an oral medication called Riluzole (brand name Rilutek); this medication has been shown to slow the progression of ALS and increase patient survival time, potentially by attenuating the negative effects on motor neurons of the increased glutamate (an excitatory neurotransmitter) levels in these cases [8, 9, 12]. For some patients whose breathing is impaired as a result of the disease, non-invasive positive pressure ventilation has been used, and one study showed a median survival time of 18 months for these patients versus 6 months for those that did not tolerate the treatment [24].

ALS is one of several diseases in which the pathology seems to be associated with abnormal protein aggregation affecting normal cellular functioning. In the specific case of ALS, the misfolded, aggregating protein that has been extensively studied and utilized in experimental models is superoxide dismutase 1 or SOD1, although it has only been observed to account for about 20% of fALS cases and about 2% of all ALS cases [6, 3]. Researchers have identified 150 distinct mutations in the SOD1 gene. It usually exhibits an autosomal dominant inheritance pattern, and it encodes a protein involved in the cellular response to oxidative stress, specifically through its mediation of the conversion of superoxide radicals to hydrogen peroxide [3]. The original postulation that the loss of SOD1 function contributes to defective cellular stress response in ALS pathogenesis has been replaced by the idea that there is a toxic gain of function regarding this protein; in conjunction with aggregation of misfolded peptides, the decreased *proper* functioning of SOD1 may be contributing to motor neuron degeneration [1]. As discussed below, misfolded proteins are processed and degraded by the ubiquitin-proteasome system, and it is possible that the UPS is compromised to an extent in ALS. One group has noted that the proteins which comprise aggregates such as the SOD1 inclusions in ALS are often linked to the critical UPS protein ubiquitin; their research paper also includes evidence from transgenic mouse studies which correlates levels of mutant SOD1 aggregates with disease development [2]. Our laboratory examines the link between SOD1 aggregation and different components of the UPS, including the focus of some of the experiments I have worked on, the deubiquitinating enzyme USP7.

Our lab has worked with a mutant form of the protein SOD1 that was generated to include a single base pair substitution previously identified in patients. We have also

used this model to study a few other aggregate-forming proteins that have been linked to ALS in recent years. One of these proteins is Tar DNA-binding protein, or TDP-43, an RNA/DNA-binding protein that normally functions within the nucleus [3]. Mutations in the TDP-43 gene have been identified in about 4% of fALS cases in addition to being observed in some sALS cases. Mutations in another RNA/DNA-binding protein, FUS, have been correlated with this disease in 1-2% of familial cases and we are currently working with several mutant genetic constructs containing both TDP-43 and FUS in the *C. elegans* worm and HEK293 mammalian cell culture models to study ALS pathogenesis [3]. In discussing TDP-43 and FUS in their paper, one research group raises the point that the regulatory role of these proteins in gene expression, particularly within the context of cellular stress responses, could factor into the motor neuron defects observed in ALS. The connection between the regulation of gene expression and ALS will be further discussed in the examination of the role of USP7, and while these different proteins may not fit together into a clear model of pathogenesis at this time, their ties to related cellular processes warrant further investigation [3].

Ubiquitin Proteasome System (UPS) Background

Given the link between ALS and misfolded, aggregated proteins such as SOD1, TDP-43, and FUS, cellular components that are involved in protein quality control and degradation, in particular the ubiquitin proteasome system (UPS), have also been identified as potentially having a role in the pathological mechanisms underlying this disease. The UPS is a cellular pathway that regulates the expression of properly folded and functioning proteins, and its role within the cell includes targeting defective proteins (in addition to short-lived regulatory molecules) to a degradative structure known as the

proteasome [2]. Misfolded proteins are targeted to the proteasome by being attached at specific residues to the protein ubiquitin, notably at lysines that are conserved at amino acid positions 48 and 63 [5]. Ubiquitin is a 76 amino acid, 8.5 kD protein that can form chains [5]. It is important to note that there is variability within the process of ubiquitination, as the ultimate effect on targeted proteins depends upon factors such as the length and attachment sites of ubiquitin chains [2]. More specifically, polyubiquitination of proteins has been linked to the UPS pathway while monoubiquitination has been shown to induce endocytotic, DNA regulatory, and other cellular pathways [2, 7].

While the ultimate fate of a protein can be determined by general properties such as the length of ubiquitin chain attachment, there is a great deal of regulation and specificity that control the process of ubiquitination. This fact seems quite logical given that there are several classes of enzymes (and many different proteins within these groups) that are involved in ubiquitination and deubiquitination. The group of proteins involved in the UPS can be activated by stimuli such as oxidative stress. In this specific case, the transcription of genes for UPS components as well as antioxidant detoxification enzymes is upregulated by the binding of Nrf2 (released from its inhibitory interaction with Keap1 in the cytoplasm) to antioxidant response elements (ARE) [2].

Another important aspect of proper UPS functioning is proteasomal targeting, a process that involves a collection of enzymes attaching a ubiquitin chain to the defective protein. The first step in this process involves the ubiquitin-activating or E1 enzyme which binds and adenylates ubiquitin, preparing it for transfer to the next enzyme in the pathway, the ubiquitin-conjugating E2 enzyme. The E3 ligases subsequently play a role

in linking the ubiquitin molecules to the proteins at lysine residues. In some cases, the ubiquitin chain is extended by E4 enzymes, and the polyubiquitin chain serves as a signal for transport to the UPS as previously discussed. It is important to note there are hundreds of E3 ligases with different substrate specificities, a regulatory aspect of the UPS system that also extends to some of its other components. In addition to these aforementioned enzymes, there is also a class of proteins called the heat shock proteins (HSP's) whose activity is induced in response to cellular stresses. The roles of HSP's (also known as chaperones) include attempting to refold misfolded proteins as well as assisting in their targeting to the proteasome for degradation [2].

When proteins are tagged with the appropriate polyubiquitin signal for degradation, they are transported to the organelle where this process takes place – the proteasome. The size of the proteasomes based on sedimentation assays is 26S, and they have been described as being barrel-shaped. These structures are found in both the nucleus and the cytoplasm, and they contain degradative proteins that act upon targets including proteins that are oxidized or misfolded, as well as short-lived regulatory molecules whose level of functioning within the cell must be controlled [2, 5]. These are essential cellular functions, and given our discussion of misfolded proteins in the case of ALS, it should seem reasonable that a link has been drawn between defects associated with the UPS and this disease, specifically the familial form as described within a recent paper covering this topic [2]. Our lab has run several experiments within the past year on certain components of the UPS, such as heat shock proteins, E3 ligases, and the focus of the next topic of discussion, the deubiquitinating enzymes.

Deubiquitinating Enzyme

The deubiquitinating enzymes (or DUBs) are members of two protease families, a characterization which points towards their role in cleaving protein components – specifically the attached ubiquitin molecules that serve as targeting signals. These two families are the metallo-proteases and the cysteine proteases, with the latter group including the majority of deubiquitinating enzymes. The active site of the cysteine protease deubiquitinating enzymes consists of a catalytic triad, a commonly observed feature in proteases; in this specific case, the triad consists of aspartate, histidine, and cysteine residues, and this multi-step reaction which alternately utilizes these different amino acid components leads to the cleavage of ubiquitin from the rest of the ubiquitin chain or the main protein itself. As further noted within a study on the topic, "The cysteine protease DUBs can be further organized into four subclasses based on their Ub-protease domains: ubiquitin-specific protease (USP), ubiquitin C-terminal hydrolase (UCH), Otubain protease (OUT), and Machado-Joseph disease protease (MJD)" [10]. The USP group is composed of over 60 enzymes making it the largest of the DUBs, and it includes the protein USP7 that has drawn the interest of labs (such as our own) that have been researching neurodegenerative disorders [11]. It was mentioned previously that researchers have observed specificity in the interactions between DUBs and the proteins they act upon – a concept that we will examine with regards to USP7 – and this facet of DUB functioning may be attributable in the case of the USP's to the various N and C terminal extensions that exist on this group of enzymes [11]. Even if all of the specific interactions and binding partners of DUBs such as USP7 have not been elucidated, we can still speculate on the significance of alterations in the activity levels of

these enzymes in disease states such as ALS. These hypotheses are driven in part by the known functions of DUBs in balancing the activity of other components of the UPS, an example of which is recycling ubiquitin molecules [4, 5]. In the specific case of USP7 which is being examined in this paper, the hypotheses regarding this protein's role in ALS pathology will also be based upon previous research on its role in other biochemical contexts.

USP7 Background

One of the interesting aspects of ubiquitin-specific protease 7 (USP7) is its potential role in several different cellular pathways. The apparent multi-functionality of this enzyme is even encompassed by its name, as USP7 is also referred to as herpes-associated USP (HAUSP) based on the discovery that it can interact with the herpes virus E3 ligase ICP0 [10]. This finding has been examined further in recent years so that the effects of USP7 expression on herpes viral protein levels could be better understood [29]. Several studies have also reported on interactions between USP7 and various proteins that are not related to the herpes virus [13].

USP7 is a protein of approximately 130 kDa (1102 amino acids) that is encoded on the short arm of human chromosome 16 [14, 15]. One unique feature of USP7 is that it is the only member of the USP family of proteins that contains a MATH33 (meprin and TRAF homology) domain [10]. The TRAF-like domain is also known as the tumor necrosis factor-receptor associated factor-like domain, and in USP7 it consists of an 8-stranded anti-parallel beta-sandwich structure with a surface groove in the middle that is critical in the binding of this protein to others such as p53 and Mdm2, important interactions that will be further discussed later in this paper [11].

Our lab identified USP7 as a protein of interest in a *C. elegans* worm genetic screening experiment that utilized small interfering RNAs (siRNAs). This experiment involved placing these worms expressing the SOD1 G85R mutant transgene, which is commonly used in our lab to study ALS-related pathology, on bacterial lawns expressing different siRNAs to cause the knockdown of expression of specific genes, with each siRNA targeting one gene. The goal of this experiment was to identify other genes that may be implicated in disease development. The mSOD1 proteins were tagged with yellow fluorescent protein (YFP), and the expression patterns and aggregation levels of mSOD1 specifically in neurons were tested through the use of a pan-neuronal promoter called synaptobrevin-1 (snb-1) in association with the transgene. The assessment of the potential effects of ALS-related pathological conditions on a cellular level can be done effectively in *C. elegans*, as health measures such as thrashing and survival can be observed, in addition to the aggregation of fluorescently-tagged proteins [6].

Worms being grown on siRNA strains that drew the researchers' interest were further studied through the use of a biochemical fractionation assay (which will be detailed in the data and analysis section) so that aggregation levels of mSOD1 could be more clearly determined. One of the results of these investigations was USP7 being identified as a protein of interest, as there was a reduction in the aggregates in worms that had been fed with the bacterial strain carrying the siRNA specific for this enzyme [6].

Since the completion of this particular study, our laboratory has continued to investigate the effects of different expression levels of USP7 (as well as other enzymes that function within the UPS) on the formation or reduction of protein aggregates. While our lab has obtained some interesting results in relation to this topic that will be discussed

in this paper, the task of elucidating the specific pathways involving USP7 that may be affecting aggregate formation still remains. In addition to interpreting our own data, we may also be able to gain insight on the potential function of USP7 within the context of ALS from previous studies that have focused on this protein.

Much of the previous research regarding USP7 has focused on its relation to tumor suppressor proteins such as p53 and FOXO4, but one exception to this trend is a 2002 paper that examines USP7 within the context of another neurodegenerative disease – spinocerebellar ataxia type 1 (SCA1). The pathology of SCA1 is related to mutations that affect the protein ataxin-1, specifically an increase in polyglutamine (CAG) repeats in the gene sequence. This research group's use of several assays including yeast hybrid screening and coimmunoprecipitation led to the identification of USP7 as a binding partner with ataxin-1. This paper concludes that the decreased affinity of USP7 for mutant ataxin-1 versus the wild type form may have implications regarding the development of SCA1. The authors posit that USP7 may normally function to target defective ataxin-1 proteins for proteasomal degradation through ubiquitin chain cleavage, and that this pathway may be compromised with regards to the mutant form of ataxin-1. There are some parallels between SCA1 and ALS, as both are neurodegenerative diseases in which it seems that abnormal proteins are involved in pathological processes that eventually result in motor neuron death. While these generalizations could be applied to several other diseases, a fact that is mentioned in the paper currently being discussed, the idea regarding USP7 directly binding with the defective protein warrants further consideration [15]. A possible parallel situation in ALS in which USP7 may bind to proteins such as SOD1 or TDP43 will be explored later in this paper.

Several research papers have been published over the last decade focusing on the link between USP7 and proteins that are in some way related to the processes of cellular damage response and cell cycle regulation. In particular, researchers have obtained results that have allowed them to elucidate a pathway involving USP7, Mdm2 (an E3 ligase), and the tumor suppressor protein p53 [13]. This latter protein is often discussed within the context of cancer development, but alterations in its activity levels could very well be related to other pathology states. It functions as a key regulator of the cell cycle, and it is the manipulations of the activity of proteins like p53 (such as the tumor suppressor INK4α) that allow the cell to either grow and develop or respond to adverse conditions, a process that often includes "a senescence-like proliferative arrest," at the appropriate times [16]. P53 is stimulated in response to DNA damage, and evidence has shown that its transcriptional activation of the gene for the protein p21 (a Cyclin-dependent kinase inhibitor, or CKI) can lead to cell cycle arrest in the G_1 phase [17]. These are some of the key components and steps of cell cycle regulation, but the complexity of the entire picture and the applications of this system (especially with regards to our focus on ALS) can be better appreciated if we include other factors such as the role of USP7 in the discussion.

The link between USP7 and p53 has been investigated by several research groups. The authors of one such paper discuss the results of previous research which had revealed that USP7 interacts not only with p53, but also the E3 ligase Mdm2. The latter is a protein that had been previously shown to modulate p53 activity at both the transcriptional and post-translational levels [11, 13]. This group conducted several experiments designed to identify the specific binding regions between USP7 and both

p53 and Mdm2, and their results helped build upon a model that indicates a regulatory role of USP7 on the activity of p53. They determined through gel filtration chromatography the binding residues within both the TRAF-like domain of USP7 and p53, and they did the same for this region of USP7 and Mdm2. They also performed a competitive binding assay to better understand this system in which USP7 seemed to bind to and stabilize both p53 and its inhibitory regulator, Mdm2. The results of this experiment helped this research group build upon the model for the interactions between these three proteins, as it was shown that USP7 shows preferential binding to Mdm2 even when there was a ten-fold excess of p53 present. This result was further supported when the results of their isothermal titration calorimetry experiment showed a binding affinity between USP7 and the Mdm2 substrate that was 7 times the size of the corresponding value for USP7 and p53. The researchers conclude that their data supports a model in which HAUSP/USP7 binding to and stabilization of Mdm2 is the physiologically significant reaction compared to binding of USP7 and p53 [11]. In this model which has been further supported and detailed in several other studies, Mdm2 is stabilized by USP7-mediated deubiquitination, and this stabilization allows it to ubiquitinate and inhibit p53 [11, 13]. This concept of the knockdown of USP7 activity affecting important cellular pathways has emerged in several different situations, and it is especially interesting that a similar effect was noted in the study of another tumor suppressor protein – FOXO4 [7].

As is demonstrated and explicitly stated by a recent group's study, the parallels between FOXO4 (a forkhead box O transcription factor) and p53 extend beyond their common roles as tumor suppressor proteins that are involved in cell cycle regulation. This research team discovered through their work on FOXO4 that this protein is post-

translationally regulated through a specific binding interaction with USP7, as was the case for p53. Just as it did with p53, USP7 downregulates the activity of FOXO4, but this study presents data on what seems to be an added dimension within this particular regulatory system that relates to the kinetic responses of the involved enzymes. In addition to determining that FOXO4 is monoubiquitinated and translocated to the nucleus in response to hydrogen peroxide-induced oxidative stress conditions, this group identified USP7 as a binding partner and downstream regulator of FOXO4. These relationships to USP7 were determined through a yeast two-hybrid screen and subsequent experiments in which the effect of different levels of this DUB (as well as USP14 as a control to support the specificity of the FOXO4-USP7 interaction) on monoubiquitinated FOXO4 was tested. The data obtained in this study was used to develop a model that can be briefly summarized within the following steps:

1. Oxidative stress induces monoubiquitination of FOXO4 by an E3 ligase.
2. Monoubiquitinated FOXO4 is translocated to the nucleus.
3. FOXO4 activity "enable[s] cells to arrest in the G1 phase of the cell cycle to prevent further oxidative damage before resuming the cycle."
4. USP7 deubiquitinates and inactivates FOXO4 in a reaction that is initiated and conducted more slowly than the monoubiquitinating, activating reaction between FOXO4 and the E3 ligase.

The authors of this paper hypothesize that their data and this model regarding USP7 is indicative of "stress regulation of FOXO4," and this idea of USP7 tempering the cellular response under stressful conditions (in this case, through temporal control of FOXO4 activity) is especially interesting when we consider the data our lab and others have

gathered [7]. Is it possible that the inhibition of USP7 is providing damaged cells with a more substantial stress response that is beneficial for combating the acute pathology? This idea will be discussed further later in this paper.

The FOXO4 tumor suppressor pathway is mentioned in another paper that focuses upon a potential application for the results obtained from all of the aforementioned studies, namely the therapeutic inhibition of components of the UPS. In their 2007 review article, Guedat and Colland specifically discuss this idea within the context of cancer treatment, as they describe an oncogenic pathway (PI3K/PKB) that can potentially be downregulated by inhibiting USP7 activity given this DUB's actions on FOXO4. They cite a specific example of a USP7 inhibitor, the synthetic molecule HBX 41, 108, which had demonstrated the hypothesized activity relating to p53 function and tumor suppression in HCT116 colon cancer cells [4]. We have utilized this molecule to study the effects of USP7 knockdown within our context of studying ALS pathology, and our results which are depicted in Figure 1 indicate that inhibition of USP7 led to a decrease in protein aggregates (this can be clearly seen in the insoluble P2 fraction image on the right for when 10 μM HBX 41,108 was added to cells).

While results such as this may seem promising in terms of the significance of USP7 in ALS research and its potential role as a therapeutic target, there is still much work to be done to reconfirm and better understand this observed effect. We have investigated the role of USP7 in ALS pathology, and our experiments will be discussed in the next section of this paper. Just as with the previous studies that have been covered here, our data seems to show that altering USP7 levels has some sort of effect on the cellular response to a stressed state. However, we must still identify which of the

multiple pathways that include USP7 may be involved in this case, and assess the nature and degree of its relation to the aggregation pathology in ALS (a concept which itself must be further examined as previously stated).

The key result that brought the potential role of USP7 in ALS pathology to our lab's attention came from a 2009 study involving our lab's principal investigator. The initial focus of the study was on the effects of aggregated mSOD1-G85R proteins on neuronal functioning and on a broader level the locomotion and viability observed in *C. elegans* worms. Experiments involving transgenic animals expressing mSOD1-G85R yielded convincing results regarding the relationship between this specific mutation and an ALS-like phenotype. Wild-type control and mutant worms expressing YFP (linked to the SOD1 transgene in each case) were compared in terms of their forward movement and thrashing, and it was found that the G85R worms were markedly deficient in both of these categories compared to the wild-type gene-expressing worms. This difference in functioning can be better understood based on the experimental observations at the cellular level which supported the hypothesized effect of protein aggregation and neuronal dysfunction stemming from the G85R mutation. Both fluorescent and electron microscopy demonstrated the dense accumulation of protein aggregates in the mutant worms compared against the wild-type controls in which YFP-derived fluorescence was more evenly distributed [6]. This observation was also supported by the results of FRAP (fluorescent recovery after photobleaching) experiments; recovery time for fluorescence after photobleaching was more prolonged in G85R worms, an indication of aggregate formation [6, 18].

The research team also performed biochemical fractionation to investigate this potential pathophysiological phenomenon relating to G85R proteins. This is an important technique that we have used repeatedly in our studies of ALS, and it will be further described in the forthcoming discussion of our experiments relating to USP7. To summarize, it involves the separation of cellular components into soluble and insoluble fractions with the goal of determining whether or not insoluble aggregates are being formed in a particular transgenic cell type. As was seen in other experiments, G85R worms (expressing ALS phenotype) were shown to possess aggregates of this mutant protein based on biochemical fractionation and subsequent Western blotting. The imaging derived from this assay showed a strong band corresponding to the SOD1-G85R-YFP polypeptide within the P (insoluble) fraction for the mutant transgenic worms, while no such band was found in the same fraction for the WTSOD1-YFP worms. With regards to neuronal abnormalities, it was observed through electron microscopy that neurons in the mutant worms possessed relatively fewer organelles, axons with smaller diameters, and fewer synaptic vesicles compared to the wild-type controls. In addition to these promising results seen in *C. elegans* relating the G85R mutation to an ALS-like phenotype and observable cellular defects, this study describes how a similar relationship was observed in mice that were injected with this mutant SOD1 transgene, while wild-type control mice did not exhibit such symptoms [6].

After having established this strong link between the G85R mutation and the ALS-like phenotype, this research group focused on proteins that might modify this effect of mSOD1 aggregation and neuronal dysfunction, and these experiments led to the identification of several candidates for study in our lab. The mSOD1-G85R YFP-labeled

worms were placed on plates covered with bacterial feeding lawns that were expressing different RNAi strains, and the researchers made note of worms in which increased fluorescent aggregation and diminished health (or vice versa) were observed. Amongst the group of genes that drew attention based on this procedure was USP7, a protein whose decreased expression was uniquely correlated with a reduction in protein aggregation AND improved health of the animal [6].

This result prompted our lab to continue investigating USP7, a task that was primarily undertaken by one of our postdoctoral researchers whose experiments paved the way for my subsequent work in the lab. In order to corroborate the result previous result regarding knockdown of USP7 expression and a corresponding reduction of protein aggregates in G85R worms, this researcher utilized the biochemical fractionation assay within human transgenic cells [6]. After the preparation of the appropriate gene products through DNA subcloning, this experiment was ready to be conducted.

Once the biochemical fractionation was completed, the resulting soluble and insoluble fractions were run on a Western blot gel along with control samples to determine the expression levels of our proteins of interest. As can be seen in Figure 2, a postdoctoral researcher in our group was able to substantiate the previous result regarding the reduced expression of USP7 and a corresponding reduction in aggregate formation, this time within the context of mammalian cells, specifically those derived from a human embryonic kidney cell line [6].

A clear distinction exists in this image between the levels of mSOD1-G85R protein expression within the P2 (insoluble fraction) samples from cells in which control shRNA was used compared to those transfected with a short hairpin (sh)USP7 construct.

Just as was seen in previous experiments, knockdown of USP7 expression has been shown here to cause a reduction in SOD1-G85R protein aggregates [6]. While speculation about the potential cause of this observation could follow this result, it was important to gather more evidence in support of a direct correlation between USP7 expression and SOD1-G85R aggregation. To work towards this goal, the postdoctoral researcher who obtained these results devised a rescue experiment in which cells were co-transfected with SOD1-G85R, an shUSP7 construct, and a knockdown-resistant shUSP7 construct. This is termed a rescue experiment because the knockdown-resistant (KDR) shUSP7 construct is testing whether or not the original phenotype observed in SOD1-G85R cells (which normally express endogenous USP7) can be "rescued" after expression of this gene has been knocked down. Observing normal levels of aggregation in these cells co-transfected with the shUSP7 and shUSP7.KDR constructs would support a correlation between USP7 expression levels and SOD1-G85R aggregation. The DNA subcloning projects leading up to this experiment (in addition to others unrelated to USP7) comprised a significant portion of my laboratory work, and this process included many unsuccessful attempts and necessary adjustments before the final genetic constructs were obtained.

Materials and Methods

RFP.shUSP7 Subcloning Procedures

The synthesis of our RFP.shUSP7 gene product that would be used as an experimental control began with the preparation of the RFP plasmid backbone. We performed restriction digest cuts on our lab stock RFP plasmid using the enzymes BamH1HF and HindIII. The obtainment of the appropriate digested RFP backbone was confirmed via SDS-PAGE analysis, and this plasmid DNA was then isolated by gel extraction and stored for later use.

The next step of the subcloning process involved the generation of the shRNA insert specific for USP7 that would be ligated into the restriction cut RFP plasmid. The shUSP7 insert was designed to specifically bind to and inhibit the transcription of the endogenous USP7 gene, and the BamH1 and HindIII restriction cut sites were also included in this gene product. The shUSP7 RNA strands were ordered and after being annealed to each other, DNA ligation was performed with the RFP.BamH1HF.HindIII cut plasmid backbone with DNA ligase.

Amplification of the newly generated RFP.shUSP7 construct for use in the mammalian cell model was achieved via bacterial transformation and subsequent DNA isolation. Antibiotic selection was utilized to grow colonies containing our gene product, as the RFP backbone contained a resistance gene specific for chloramphenicol that was added to the bacterial growth media. Our RFP.shUSP7 plasmid construct was isolated from the bacterial inoculates using the DNA MINI prep assay. Following this step, we

confirmed that the appropriate gene product had been obtained by performing restriction cuts and subsequent SDS-PAGE analysis. DNA samples that tested positive based on SDS-PAGE band analysis were then prepared and sent to the GENEWIZ laboratory for sequencing analysis, the results of which were then compared to the known sequences of our shUSP7 insert and the RFP backbone. Once we confirmed a positive DNA sample based on sequencing analysis, we performed an additional amplification step using a large volume of bacterial inoculates and subsequent DNA isolation via the MIDI prep assay. The resulting eluted samples containing our target RFP.shUSP7 construct were stored at -20^{o} C for eventual use in subsequent experiments including the shUSP7 rescue experiment.

pCI/USP7.KDR Subcloning Procedures

The shUSP7 rescue experiment necessitated the generation of a gene product that would introduce exogenous, knockdown-resistant USP7 into mammalian cells that were co-transfected with the RFP.shUSP7 construct as well as mSOD1-G85R, with the ultimate goal of restoring the mSOD1-G85R aggregate phenotype observed in cells expressing endogenous USP7. The initial steps of this process involved a PCR protocol designed for site-directed mutagenesis, an assay called overlap-extension PCR (OE-PCR). This protocol involves an initial set of PCR reactions that generate genetic products with overlapping ends, followed by a second PCR reaction in which the initial products are annealed and then used as the DNA template. This technique is useful for introducing point mutations at specified sites within a gene [19, 20].

The primers we designed and ordered for this protocol met a few key specifications. The first important aspect of designing these primers was ensuring that site-directed mutagenesis within the USP7 sequence was induced in such a way that the amino acid sequence of this protein would not be altered, but the product would not be recognized and bound by our RFP.shUSP7 construct. The second important specification for these primers was including restriction cut sites that would allow for the eventual ligation of this USP7 insert into the pCI.FLAG plasmid backbone. The OE-PCR protocol we followed utilizing the four primers that were designed is depicted in Figure 3. The USP7 template that was used for this assay was obtained from a lab stock and was labeled pCI.Flag.HAUSP (recall that HAUSP is an alternative name for USP7).

Following first PCR reaction included in the OE-PCR protocol, the obtainment of the proper genetic products was confirmed by SDS-PAGE band analysis. The appropriate DNA constructs were then extracted and purified from the SDS-PAGE gels and eluted in 50 μL buffer. The second OE-PCR reaction was then performed using the DNA products from reaction 1 (following their being annealed together) as the new template, as well as the FlagUSP7BclIF and FlagUSP7EcoRVR primers. Following this second OE-PCR step, a reaction was prepared using the OE-PCR DNA product, Taq Polymerase, buffer, and water to add "sticky ends" at both termini of the gene product to facilitate the following subcloning steps. These components were mixed and placed at 72^{o} C for 20 minutes. Once this reaction was run to completion, we performed SDS-PAGE band analysis to confirm the generation of our desired construct and subsequently extracted and purified the USP7 knockdown resistant (KDR) DNA insert which was eluted in buffer.

The next step involved the use of an assay called TOPO® PCR cloning, a technique that would allow us to more easily identify bacterial colonies that had been successfully transformed with our USP7.KDR construct and thereby facilitate the subcloning process. This assay involves a short reaction that inserts our USP7.KDR product from the OE-PCR into a specific vector labeled PCRTOPO. The resultant PCRTOPO.USP7 product has two important properties which comprise the beneficial nature of this assay. The first is that the USP7.KDR insert contains a gene coding for antibiotic resistance to ampicillin (AMP), and thus growth media containing AMP could be used to select for transformed bacterial colonies containing our plasmid. The second property is that bacterial colonies that contained the *successfully*-ligated PCRTOPO and USP7.KDR DNA products would appear blue on growth media that included X-Galactose (X-Gal), while colonies containing cells in which DNA insertion was not successful would appear white [21].

This assay involved mixing a small quantity of the OE-PCR USP7.KDR DNA with the PCRTOPO vector, an aliquot of bacterial cells, and a salt solution. Following heat shock transformation and bacterial inoculation in SOC growth medium, an AMP+X-Gal plate was used as the growth medium for bacterial colonies. Several blue colonies were picked from the plate following overnight incubation at 37^{o} C, and these colonies were then inoculated in SOC+AMP in preparation for a DNA MINI prep assay. A group of the samples obtained from this DNA isolation assay were sent for sequencing analysis which confirmed the presence of a positive PCRTOPO.USP7KDR clone. An aliquot of the remaining bacterial inoculate from this positive sample that had been used in preparation for the previous MINI prep step was added to a larger volume of growth

media (60 mL's of LB+AMP) and inoculated overnight at 37^{o} C. This bacterial inoculate was then used for a MIDI prep assay that allowed for amplification of our DNA construct.

The final step of the subcloning process involved transferring the USP7.KDR insert into the desired background vector - pCI.Flag.HAUSP – for our rescue experiment. Restriction digests were set up for both of these gene products using the enzymes PflMI and EcoRV, and CIP was added to each reaction tube following digestion to remove terminal phosphates from the DNA strands and thus prevent re-ligation. The digested pCI.Flag.HAUSP and USP7.KDR constructs were then ligated at 16^{o} C overnight using the enzyme DNA ligase. Following this ligation, bacterial transformation and inoculation were performed in preparation for DNA MINI preps. Once the plasmid DNA was isolated, restriction cuts with the enzyme DraI were performed followed by SDS-PAGE band analysis to determine if any positive pCI/USP7.KDR clones had been obtained. Samples that tested positive by DraI restriction digest analysis were then sent for DNA sequencing which ultimately confirmed that we had successfully generated our desired DNA construct containing the USP7.KDR insert within the pCI.Flag.HAUSP vector backbone. The bacteria from the positive clone were inoculated in 60 mL's of LB+AMP in preparation for MIDI prep amplification, and the plasmid DNA isolated from this assay was stored at -20^{o} C for eventual use in the USP7.KDR rescue experiment.

Biochemical Fractionation and Western Blot Analysis

Biochemical fractionation is a multiple-step process that begins with the transfection of the genetic constructs into the cellular environment within which they will

be examined. In this particular case, an shRNA (or small hairpin RNA) construct specific for the USP7 gene was used in order to knock down its expression in the transfected cells. The shUSP7 construct was co-transfected with an mSOD1-G85R construct so that the effect of USP7 knockdown on aggregate formation (induced by the G85R protein) could be studied. The cell line used for these initial experiments involving USP7 (as well as later experiments involving this gene) was a human embryonic kidney cell line (HEK293). These cells were equally distributed amongst four plates representing our samples for the USP7.KDR rescue experiment. After we prepared a DNA mix containing the BOS-SOD1^{G85R} construct (which would form aggregates) as well as OMEM growth medium, we pipetted equal amounts into four tubes. We then added the plasmids that would define each experimental sample as follows: Sample 1 – RFP.shCTRL+pCI.GFP, Sample 2 – RFP.shCTRL+pCI/USP7.KDR.MIDI2, Sample 3 – RFP.shUSP7.1+pCI.GFP, and Sample 4 – RFP.shUSP7.1+pCI/USP7.KDR.MIDI2. The next step was to prepare a Lipofectamine mix, and after aliquots of this solution were added to each DNA sample and these tubes were incubated for approximately 17 minutes, they were plated in the dishes containing OMEM. These dishes were incubated at 37º C for approximately 20 hours, at which time the medium was replaced with DMEM/10. The samples were then placed back into the incubator for approximately 70 hours.

After the transfections and subsequent cell culturing were completed, the next step in this assay was the lysis of the cells through the use of a mild detergent. Once the cells were collected and the lysis buffer was added, a process called sonication was employed which involved exposing the cells to a high frequency sound and thereby

contributing to the separation of cellular components. The samples were placed in the sonicator for 5 minutes, although this process had to be repeated for samples 1B-4B. This technique was followed by ultra-centrifugation, as the sonicated samples were transferred to ultra-centrifuge tubes, balanced by their masses, and then placed in the Airfuge and spun at approximately 25,000 PSI for a period of 5-10 minutes.

At this point in the biochemical fractionation assay, the samples contained a pellet and supernatant, with the latter representing the soluble (S) fraction within which the non-aggregated proteins being expressed in the cells could be found. The supernatant was pipetted into fresh tubes which were appropriately labeled as the S1 samples. The final step of the fractionation was the isolation of the insoluble (P) fraction. Each of the pellets from the previous sample were once again mixed with a mild detergent, exposed to sonication (this time for 10 minutes), washed and then ultra-centrifuged. The resulting pellets were then resuspended in a urea/SDS solution, sonicated one final time, and the supernatant for each sample (now representing the insoluble or P2 fraction) was pipetted into a fresh tube and stored.

Once the biochemical fractionation was completed, the resulting soluble and insoluble fractions were almost ready to be run on a Western blot gel along with control samples to determine the expression levels of our proteins of interest. To prepare for this assay, we first had to measure the protein concentration of each sample. We did this by performing a BCA assay, a process that involved the preparation of a 96 well plate containing aliquots of a blank solution and our S1 and P2 samples – each mixed with water – as well as several standard solution samples of varying concentrations (which were used to generate a standard curve). After preparing the wells which all contained 12

µL total of solution (10 µL of water+ 2µL of the blank solution or fractionation sample, or 12 µL of the standard solution), we added 200 µL of a mixture containing Buffer A and Buffer B in a 50:1 ratio to each sample. This plate was then incubated at 37º C for approximately 20 minutes, and the protein concentrations were measured using the Hybrid Reader, a machine that utilizes the standard curve to comparatively determine the concentrations of the S1 and P2 protein samples.

Once the concentrations had been measured, aliquots of the S1 and P2 samples were combined with their appropriate buffers (Buffer B for S1 and urea buffer for P2) as well as 4X loading buffer to reach final protein concentrations of 2 µg/µL for the S1 samples and 1 µg/µL for the P2 samples. After incubating the mixed samples at 95º C for approximately 10 minutes, they were loaded onto two separate gels – one containing the S1 samples and the other containing the P2 samples. Once this run was completed, the gels were transferred to membranes and then incubated in a solution of 5% milk in TBS-T for one hour. The milk was washed off following this incubation with TBS-T, and both of the membranes were treated with a primary antibody solution overnight. The primary antibodies used were rabbit anti-SOD1 1-100 (1:3000 dilution) and mouse anti-actin C4 (1:5000 dilution). The following day we removed the primary antibody, washed the membranes in TBS-T and then incubated them for one hour with a pair of secondary antibodies – donkey anti-rabbit-800 (1:20,000 dilution) and donkey anti-mouse-680 (1:30,000 dilution). The membranes were then washed with TBS-T four times for 10 minutes each, and then with TBS twice for five minutes each time. Following these washes, the membranes were placed in an imaging device within which they were scanned so that our final results could be analyzed. Images were created which

specifically depicted fluorescence derived from bands corresponding to the actin proteins within our S1 samples (a control) as well as our primary result of interest for this experiment – the mSOD1 bands within both the S1 and P2 samples.

Microarray Analysis

A microarray analysis was conducted in which the expression levels of genes in cells containing an shUSP7 construct were compared to those in cells containing a control shRNA product (shCTRL). A microarray grid – the Human Gene 1.0 Affymetrix array – was obtained which consisted of squares in designated locations, with each containing complementary DNA (cDNA) specific for a certain cellular gene. The idea behind this experiment was to apply both the shUSP7 and shCTRL samples to the microarray grid after the two were labeled with either red or green fluorescent tags. The shRNA samples contained mRNA transcripts corresponding to the genes within the microarray grid, but it was expected that the amounts of these transcripts (which indicate gene expression levels) would differ between them. These differences would be indicated within this assay when the samples were applied to the grid and the labeled mRNA transcripts hybridized with their cDNA binding partner. Assuming that the shUSP7 sample was labeled red and the shCTRL sample green, the squares would appear red for genes which were more highly expressed in the shUSP7-treated cells given the larger number of transcripts that would hybridize with the cDNA, and vice versa for green squares (relatively equal expression of a gene in the two cell lines would correspond to a yellow square on the microarray grid) [23].

The shUSP7 and CTRL samples were derived from HEK293 cells into which these constructs had been introduced. After RNA was extracted from the cells using an

Invitrogen TRIzol kit and then isolated with a Qiagen RNeasy kit, an Affymetrix 3' IVT Express Labeling Assay was used to generate single-stranded cDNA which were then converted into double-stranded cDNA (through the use of DNA polymerase and RNase H). The final step of this assay that contributes to the preparation of the shUSP7 and CTRL samples which would be hybridized with the Affymetrix microarray grid was to generate RNA molecules from the double-stranded cDNA. Once these RNA molecules were hybridized with the microarray grid, the Affymetrix Fluidics Station 450 kit was used for staining and washing so that gene expression levels for the two samples could be represented by red or green fluorescent labeling. Once this data was gathered, it was analyzed and organized into a table that includes information about relative expression levels between the shUSP7 and CTRL samples, p values, gene descriptions, and other statistical parameters [25, 26].

Results

Subcloning of RFP.shUSP7 construct

In order to test the overall hypothesis that an exogenous, knockdown resistant USP7 genetic construct could rescue the aggregation phenotype in cells also co-transfected with mSOD1-G85R and shUSP7, it was first necessary to generate an shUSP7 product. We specifically wanted to conduct DNA subcloning assays that would produce an shUSP7 insert expressed within the RFP backbone vector. A sample of RFP was digested with restriction enzymes in preparation for an eventual ligation to the shUSP7 insert. The digested vector DNA was isolated from this gel, purified and eluted in buffer in two separate samples – labeled RFP-1 and RFP-2 – with measured concentrations of 44.1 ng/μL and 31.3 ng/μL, respectively.

The next step of the subcloning process for the shUSP7 construct was the preparation of the shUSP7 oligonucleotide insert that would eventually be ligated with the RFP backbone. We used shUSP7 RNA products that were designed to specifically bind to the USP7 gene and inhibit its transcription (and thus the expression of the associated protein). These genetic constructs were also designed such that they contained the same restriction enzyme cut sites as our RFP backbone (specific for BamH1 and HindIII), a detail that would allow for the ligation of these molecules. After this reaction was performed to link the shUSP7 insert to a sample of the RFP-1 backbone, the DNA was amplified by bacterial transformation. These bacteria containing our genetic product were inoculated and the plasmid DNA (including RFP.shUSP7) was eventually isolated by the MINI prep assay.

The five samples obtained following the MINI prep included two (RFP.shUSP7.1 and RFPshUSP7.2) that were positive for our desired product based on restriction digest analysis. These two samples were then sent for DNA sequencing analysis, and it was found that RFP.shUSP7.1 was a positive clone. Remaining bacteria from the inoculation tube corresponding to this MINI prep DNA sample were streaked on a plate, and a single colony was then isolated and grown further so that more of this DNA could be amplified. A DNA MIDI prep was performed on this bacterial inoculate, and the isolated DNA was split into two samples with measured concentrations following elution in buffer of 5.35 ng/µL and 2886.3 ng/µL. These samples were stored at -20º C for use in subsequent experiments, including the USP7.KDR rescue experiment.

Subcloning of pCI/USP7.KDR construct

The crucial preparatory step for the USP7.KDR rescue experiment was the generation of a knockdown-resistant USP7 genetic product. The goal was to co-transfect this construct into cells with mSOD1-G85R (which would produce an aggregate, ALS-like phenotype) as well as RFP.shUSP7.1; the hypothesis behind this experiment was that our exogenous USP7.KDR product would cause a reversal of the reduced aggregation effect that had been previously observed in cells co-transfected solely with shUSP7 and mSOD1-G85R. In regards to the USP7.KDR subcloning project, the objective was to alter the DNA sequence of a USP7 genetic product so that it would express an exogenous form of this protein but it would not interact with RFP.shUSP7.1. The method employed for this experiment relied on the degeneracy of the DNA code, as single bases in the USP7 sequence that were recognized and bound to by shUSP7 could be replaced *without* altering the amino acid sequence. Primers were designed that met these specifications,

and which also included restriction cut sites – a detail that would allow us to eventually incorporate the USP7.KDR segment into a complete USP7 gene.

The subcloning assays that comprised the generation of the USP7.KDR product had to be repeated at many different points so that the appropriate components could eventually be obtained. One example of this pattern was the OE-PCR experiment at the outset; following an unsuccessful run of this experiment, we obtained a new set of primers and were then able to generate the proper DNA products without any mutations in our target sequence. The first set of PCR reactions in this two-step mutagenesis experiment was run on an SDS-PAGE gel which is imaged in Figure 3.

These samples were used as the combined template for the second OE-PCR reaction, and the DNA obtained from this next step had a measured concentration of 129.1 ng/μL. Another subcloning experiment that had to be performed multiple times was the PCR TOPO assay that was intended to introduce the USP7.KDR PCR product into the PCRTOPO background vector. We were eventually able to confirm the successful insertion of our USP7.KDR construct into this backbone by blue-white bacterial colony screening. We then isolated DNA from these bacteria that were positive for the desired PCRTOPO.USP7.KDR gene product, and we confirmed this result via DNA sequencing analysis. The sample that was positive for our construct was labeled PCRTOPO.USP7-6, and the DNA was further amplified via inoculation of remaining bacteria that had been grown for the MINI prep. The subsequent MIDI prep assay yielded a sample with a concentration of 55.4 ng/μL.

The final step of this subcloning project involved inserting the USP7.KDR sequence into its final backbone vector – pCI.Flag.HAUSP. This goal was accomplished

by restriction digestion followed by ligation of the cut DNA products. Confirming the success of these assays was first carried out by restriction digestion with the enzyme Dra1. When the proper pCI/USP7.KDR sequence was finally obtained, the Dra1 assay indicated the presence of several positive samples following the ligation step as shown in Figure 4.

Samples of the first two DNA clones (lanes 1 and 2) were sent for sequencing analysis, and the results showed that we had finally obtained our target USP7.KDR sequence within the pCI.Flag.HAUSP backbone, as sample 1 tested positive. Bacteria from sample 1 were inoculated for a DNA MIDI prep so that we could generate more of our positive genetic product. The sample that was obtained from this experiment and which would be used going forward was labeled pCI/USP7KDR6.MIDI2. Now that we had successfully generated this primary component for the USP7.KDR rescue experiment, we were prepared for the transfections of this construct and several control samples into mammalian cells. It is within this model that we would test the hypothesis that introducing an exogenous, knockdown-resistant USP7 product into cells in which this gene has been inactivated would result in the appearance ("rescue") of the mSOD1 aggregate phenotype.

Western Blot Analysis of mSOD1-G85R Aggregation Rescue in Cells Co-Transfected with pCI/USP7.KDR Construct

The RFP.shUSP7 and pCI/USP7.KDR constructs that were prepared through the subcloning experiments described in the previous sections were transfected into HEK cells along with a plasmid expressing mSOD1 so that the effects of our generated constructs on the aggregation of this mutant protein could be tested. Samples containing

four different combinations of our genetic constructs were prepared, plated so that they could transfect these cells, and incubated for approximately 90 hours. Following cell lysis and the fractionation assay, we ran the proteins from the S1 and P2 samples on a gel and then stained the membranes gathered from this gel with antibodies specific for the proteins actin and SOD1. Imaging of the bands associated with these proteins (a protein ladder was also run to confirm their presence based on their sizes) would reveal the extent of mSOD1 aggregation within the different samples. The staining of actin served as a control for protein expression within the HEK cells.

Our hypothesis regarding the effect of USP7 knockdown on mSOD1 aggregation led to the assumption that Sample 4, within which endogenous USP7 expression was knocked down but the exogenous, knockdown-resistant gene was also being introduced, would show a "rescue" of the aggregate phenotype observed in normal cells expressing simply mSOD1-G85R. We anticipated that Sample 3 (RFP.shUSP7.1+pCI.GFP) would show a reduction in mSOD1 aggregates compared to the other three samples based on previous results involving the knockdown of USP7. Samples 1 (RFP.shCTRL+pCI.GFP) and 2 (RFP.shCTRL+pCI/USP7.KDR.MIDI2) served as controls for our primary test involving Sample 4.

As can be seen in Figure 5, all of our S1 samples were positive for actin, and thus we could confidently analyze the rest of our results with an established control displaying protein expression within the HEK cells. It was expected that normal SOD1 and a small amount of mSOD1-G85R would appear by staining within the S1 samples, and this was indeed the case as shown in the bottom left image of Figure 5. The upper, bright bands within this image correspond to normal SOD1 proteins, while the lower bands that can be

more clearly seen in Samples 1 and 2 correspond to mSOD1-G85R. Most of the mSOD1-G85R aggregated proteins were expected to appear in the P2 (insoluble) fraction samples, and they are clearly exhibited in the control samples (1 and 2).

The results that are faintly depicted in the S1 SOD1 band image regarding the mSOD1 aggregates appear clearly in the P2 SOD1 band image on the bottom right of Figure 5. We predicted, based on our hypothesis, that Sample 3 would show a reduction in mSOD1-G85R aggregates compared to the control samples (1 and 2), and this was indeed the case. The bright bands in P2 Samples 1 and 2 can be contrasted with the lack of a clearly visible band in Sample 3, within which USP7 was being knocked down. The crux of our hypothesis was the prediction that Sample 4 would exhibit a restoration of the mSOD1-G85R aggregate phenotype compared to Sample 3 given the introduction of exogenous, knockdown-resistant USP7 in conjunction with the RFP.shUSP7 construct. Our results from this experiment support this claim, as a faint band corresponding to mSOD1-G85R can be seen in Sample 4, as compared to the lack of expression of this protein in Sample 3.

While our observations from Samples 3 and 4 seem at first to validate our hypothesis, the banding patterns from the control samples reveal that this conclusion cannot be reached without supplementing the results with further experiments. It can be clearly seen within the P2 samples (and somewhat less clearly within the S1 samples) that the mSOD1-G85R band appears to be stronger and brighter within Sample 2 (which includes our pCI/USP7.KDR.MIDI2 construct) as compared to Sample 1 (which includes pCI.GFP). This difference could be attributed to a direct effect of USP7 expression on mSOD1-G85R expression just as our hypothesis states; in this case, it could be argued

that overexpressing USP7 (as is done in Sample 2) can lead to an increase in mSOD1 aggregation. As explained by Dr. Goran Periz, the postdoctoral researcher overseeing this project, our experiment cannot however exclude the possibility that the observed difference in mSOD1 expression levels between the two control samples is due primarily to an inherent disparity between the rates of protein translation within the HEK cells for GFP (expressed as a control in Sample 1) and USP7 (expressed in Sample 2). This potential disparity between the translation rates of GFP and USP7 could have an effect on mSOD1 aggregate protein formation that would cause an unexpected variance between these two cell lines. It would be difficult to accurately assess the link between USP7 expression and aggregate formation as we originally sought out to do if this were the case. These results and future experiments that could help contextualize them will be covered in further depth within the "Discussion" section of this paper.

Microarray Analysis

Microarray analysis was also was performed to elucidate the role of altered USP7 expression in the formation of mSOD1 aggregates. The goal of this study was to determine how knocking down USP7 would impact the expression of other genes. While over 33,000 genes were screened for differing expression levels between a knockdown sample and a control sample (derived from HEK293 cells), this discussion will focus on the results for a select few which code for proteins of interest given their established links within previous literature to USP7 and other proteins that may be implicated in ALS pathophysiology. Several of these proteins are involved in cell cycle regulation processes, and a hypothesis regarding their interaction with USP7 and the observed effect of knockdown of this protein affecting mSOD1 aggregation will be described in the

"Discussion" section of this paper. Another hypothesis that will be explored relates to the regulation of copper levels within USP7 knockdown cells and its possible effect on SOD1 morphology and aggregation.

Before discussing the expression level results for the aforementioned group of proteins, we should establish that the microarray confirmed successful knockdown of USP7 in the cells containing shRNA specific for this gene. The data indicates that this was indeed the case, as the ratio of USP7 in the shUSP7 sample compared to the CTRL one was found to be 0.491503. The *p*-value for this result, which represents the statistical probability of observing such a data point by chance, was 2.05×10^{-7}, a value well below the normal cutoff of 0.05.

Analysis of the same statistical parameters with regards to the USP7-linked cell cycle proteins reveals a consistent and interesting pattern. As can be seen in Table 1, all of these genes were upregulated in the samples derived from shUSP7-containing cells compared to the CTRL samples. The *p*-values for all of the genes included in this table are statistically significant (<0.05). The particular mechanisms for the knockdown of USP7 potentially impacting the expression levels of these genes will be debated in the next section of this paper. It is noteworthy, however, that our results seem to corroborate the general finding within previous research that the proteins corresponding to these genes interact in some way with USP7.

The process of analyzing this microarray data also brought forth an interesting link between USP7 knockdown and the expression level of the copper-regulating protein ATP7A. In searching for mRNA transcripts whose expression levels were significantly altered in shUSP7 cells, ATP7A emerged as a gene of interest given its role in copper

homeostasis. As indicated in Table 1, this P-type ATPase involved in copper transport had a statistically significant (p-value < 0.05) expression ratio of 2.1886 in shUSP7 cells compared to control cells [36]. While the mechanism underlying this increased expression level of ATP7A requires further exploration, the alteration itself may bear significance within the context of mSOD1-G85R aggregation given the apparent effect of copper binding on the conformation of this mutant protein [31-37]. A possible model for our observed effect of reduced mSOD1-G85R aggregation in USP7 knockdown cells that involves ATP7A and changes in intracellular copper levels will be explored in the Discussion section.

The microarray result regarding ATP7A upregulation as well as the subsequent literature search that explored a possible link between ATP7A and mSOD1-G85R aggregation led to the investigation of other genes involved in copper homeostasis. The microarray results for these genes were included in Table 1; of note were the statistically significant findings that both ATP7B (another ATPase involved in copper transport and homeostasis) and COMMD1 (previously shown to impact the regulation and activity of ATP7A and ATP7B) [33, 36-37] were upregulated along with ATP7A in shUSP7 cells compared to the control cells. We observed a ratio of 1.16092 for ATP7B expression in shUSP7 cells compared to control cells and a ratio of 1.11329 for COMMD1 expression. While neither of these values represent an increase in relative protein expression level within shUSP7 cells comparable to what we observed for ATP7A (ratio of 2.1886), they could help build towards a model that explains our previous observation of reduced mSOD1-G85R aggregation in USP7 KD cells that is based on altered copper homeostasis in neurons. The other genes included in Table 1 have also been linked to copper

homeostasis in previous literature, but no statistically significant values were observed for the relative expression levels of these genes [34, 36-37].

Discussion

Previous research has implicated the protein USP7 in several cellular biochemical pathways related to tumor suppression as well as the neurodegenerative disease spinocerebellar ataxia type 1[7, 13, 15]. Our lab's work has attempted to link this protein to the pathological mechanisms underlying our main focus, the neurodegenerative disease ALS. Our investigation of this DUB was prompted by the observation from an siRNA screening assay that knockdown of USP7 leads to a reduction in mSOD1 aggregates in *C. elegans* [6]. Subsequent experiments performed by our lab involving a USP7-inhibiting drug, HBX 41, 108, as well as an shUSP7 construct corroborated this result, and we were thus prompted to further investigate this possible biochemical link.

The primary focus of my work in our lab was to perform an experiment that would validate previous results that showed that knockdown of USP7 leads to a reduction in mSOD1-G85R aggregate formation. This project was referred to as a "rescue" experiment given that we were trying to induce the reappearance of the mSOD1-G85R aggregate phenotype in cells within which aggregation had been reduced by USP7 knockdown. The hypothesis stated that introducing an exogenous, knockdown-resistant USP7 gene into mSOD1-G85R-expressing cells in which endogenous USP7 was simultaneously being knocked down by a specific shRNA construct should lead to an increase in mSOD1 protein aggregates compared to cells that had only been co-transfected with shUSP7 and mSOD1-G85R constructs. Our goal was to obtain Western blot results that would display an SOD1 banding pattern that was supportive of this claim, and thus help us build towards a causal link between altering USP7 expression and levels of mSOD1 aggregate formation.

DNA Subcloning Generated RFP.shUSP7 and pCI/USP7.KDR Constructs

The successful performance of this rescue experiment necessitated the subcloning of a pair of genetic constructs. The first one contained an shRNA insert (within the RFP plasmid vector backbone) that would specifically knockdown USP7 expression. The other construct coded for a variant of the USP7 gene such that the mRNA would not be targeted for degradation by the shRNA product due to PCR-induced single base substitutions at locations that did not affect the amino acid sequence. These two separate subcloning projects included many failed trials – particularly with regards to the USP7.KDR construct. We were, however, eventually able to validate via restriction digestion and sequencing analysis that we had successfully cloned these products within their appropriate backbone vectors (RFP for the shUSP7 construct and pCI for the USP7.KDR construct).

Relative Increase in mSOD1 Aggregation in Cells with Restored USP7 Expression

The Western blot analysis that comprised our rescue experiment made use of these two subcloning products, and having generated these constructs we were now prepared to test our hypothesis. As discussed in the previous section of this paper (Results, page 36), the banding patterns we observed after staining our membranes with an anti-SOD1 antibody were consistent with we had anticipated *to an extent*. We indeed found that introducing our knockdown-resistant USP7 construct into cells in conjunction with RFP.shUSP7 led to a relative increase in mSOD1-G85R aggregate formation compared to cells in which only RFP.shUSP7 was present. This result is indicated by Figure 5 in the "Results" section, which shows a band corresponding to mSOD1-G85R in P2 Sample 4, while this band cannot be seen clearly in Sample 3.

Our observations also raised questions that we must answer before we can definitively determine whether or not the experiment supported our hypothesis. The specific issue with our results relates to the banding pattern observed in Samples 1 and 2, both of which were experimental controls. The increased level of mSOD1-G85R aggregates in Sample 2 (containing the USP7.KDR construct) compared to Sample 1 (containing GFP) could be attributed to one of two mechanisms. The first possibility is that USP7 overexpression has an effect on mSOD1-G85R aggregate formation. This finding would seem to be in line with our original hypothesis, as we had anticipated that increasing USP7 expression in cells within which this gene had been knocked down would lead to an increase in mSOD1 aggregates. It could be argued that our results support a more general finding that includes our hypothesis – that knocking down USP7 expression leads to decreased aggregate formation – and conversely that increasing levels of this DUB leads to increased mSOD1 aggregates.

The second possibility that could explain the banding pattern from the control samples is that USP7 and GFP differ in the rate or overall amount that they utilize the cellular components which function in protein translation, and that this disparity is affecting the ability of the cells from Samples 1 and 2 to form mSOD1-G85R aggregate proteins. It is important that we ascertain which of these factors are causing the results we observed, and the postdoctoral researcher overseeing this project suggested a future experiment that could accomplish this task. This experiment would involve performing Western blot analysis of mSOD1-G85R aggregate formation in samples expressing an enzymatically-dead version of USP7 (mUSP7-C223S). The setup would be the same as it was for the experiment we conducted, and we would be able to determine if the

observed results in the control samples were attributed to the protein translation process with regards to USP7. If we were to test the same control samples but replace our pCI/USP7.KDR.MIDI2 construct in Sample 2 with mUSP7-C223S, we would expect the same results as we observed in our experiment if the second factor (regarding protein translation) was causing this banding pattern. Alternatively, if we performed this experiment with the enzymatically-dead mUSP7-C223S construct and observed a relative decrease in mSOD1 aggregate formation in Sample 2 (such that this level became closer to what is observed in Sample 1), this would indicate that the enzymatic activity of USP7 and this functional protein's expression level does have an impact on aggregate formation. Such a finding would be consistent with our hypothesis.

mSOD1 Aggregation Possibly Affected by Link between USP7 and Tumor Suppressor Proteins

In addition to the aforementioned future experiment, it would be valuable to explore biochemical pathways that could potentially underlie our hypothesized link between USP7 and mSOD1 aggregate formation. It is interesting to note the relationships that have been described in previous research studies between this DUB and proteins involved in cell cycle regulation processes. One example of this is a model that links USP7, the tumor suppressor protein p53, and Mdm2 (an E3 ligase) such that decreased USP7 activity (e.g., via gene knockdown) results in a decrease in Mdm2 activity and thus an increase in p53 activity [11, 13]. Another example involves the tumor suppressor protein FOXO4, and once again it has been observed that knockdown of USP7 results in increased activity of this cell cycle regulator [7]. The idea that our results regarding USP7 knockdown and reduction of mSOD1 aggregates could possibly

be tied to this DUB's effects on these cell cycle regulation proteins was mentioned in the "Introduction" section of this paper. While the microarray analysis our lab conducted included results for thousands of genes, the decision was made to focus on this group of USP7-associated proteins within this thesis project to see if there was evidence in support of a biochemical explanation for our observations.

The data from the microarray experiment does not provide us with a clear mechanism explaining how altering USP7 expression can directly impact these other cell cycle-associated proteins, but it does reinforce the idea that there are links between these genes. Statistically significant ratios (p-value < 0.05) comparing expression levels of genes in shUSP7 cells versus control cells were observed for p53, Mdm2, FOXO4, and CDKN1A (or p21), and all four of these genes were comparatively upregulated in the shUSP7 samples [30]. This result seems to be consistent with our expectations (given the relationships between these proteins discussed in previous literature) in the cases of p53 and FOXO4 [7, 11, 13]. Particularly in the case of FOXO4, the link with USP7 was made in a previous study at the transcriptional level, and thus the microarray analysis should serve as an accurate measure of this observed relation [7].

The result that seems to run counter to our expectations is that obtained for Mdm2; this gene was upregulated by over 47% in shUSP7 cells, and yet previous studies have indicated that USP7 knockdown results in decreased activity of Mdm2 (and thus increased activity of p53) [11, 13]. This model involving USP7, p53, and Mdm2 includes several levels of gene and protein regulation including a feedback loop that controls p53 expression via Mdm2 and separate binding of USP7 to both of these proteins [11]. It may be that our observation from the microarray analysis is due to a USP7 knockdown-

driven decrease in Mdm2 activity at the protein level (due to auto-ubiquitination and subsequent self-degradation), which in turn is leading to a compensatory upregulation of the gene specific for this protein [13].

These results highlight the difficulty in developing a biochemical model regarding ALS pathology that includes a clear impact caused by USP7. One working hypothesis that pertains to our lab's research is that knockdown of USP7 is leading to an upregulation of tumor suppressor proteins such as p53 and FOXO4, an effect that leads to an increased time window for cellular repair caused by a pathological mechanism related to mSOD1 aggregates. The upregulation of tumor suppressor proteins in response to USP7 knockdown has been discussed in several studies that have been covered within this paper. The idea of kinetics playing an important role has also been mentioned. One study portrays USP7 as playing a role in tempering the cellular response to oxidative damage that is mediated by FOXO4 activity, and the authors' research provides evidence for a temporal component to this control mechanism [7]. The importance of the "time frame" for a cellular response to damage is also discussed in a recent paper that relates USP7 activity to ERCC6, a protein that serves a critical role in transcription-coupled nucleotide excision repair (TC-NER). The authors of this study suggest that the effectiveness of TC-NER, a DNA damage repair process, may in part be a function of proteins being able to operate and assemble within an adequate amount of time [27].

Taken within our context of linking USP7 and mSOD1 aggregation, this argument regarding the potential for increased time to enhance certain cellular responses could be applied to our observations, specifically through the increased activity of tumor suppressor proteins leading to a pause of the cell cycle [7]. It could be that the cells used

in our experimental models can more effectively respond to the pathological insults associated with aggregating mSOD1 proteins under these circumstances of USP7 knockdown. This model becomes more convoluted if the functions of USP7 and SOD1 related to oxidative damage are considered as well. Both of these proteins have been shown to function in cellular repair processes related to oxidative DNA damage [13, 27]. The importance of functional USP7 within these repair processes does not seem consistent with the hypothesized model explaining our observation of reduced mSOD1 aggregates under the condition of USP7 *knockdown*. A possible explanation that could account for these various functions of USP7 is derived from the results of a study on another neurodegenerative disease – frontotemporal lobar degeneration. One group researching this topic discussed within their paper the concepts of altered apoptosis kinetics and clearance of dead neurons as affected by mutations in the gene for the protein progranulin [28]. Applying these ideas to the hypothesized model that potentially underlies our results regarding USP7 knockdown, the argument could be made that deficient damage repair in cells cotransfected with mSOD1-G85R and shUSP7 constructs is leading to increased (in terms of frequency and rate) apoptosis and clearance – an outcome that has been manifested within our results as a reduction in mSOD1 aggregates.

Hypothesis Regarding USP7-Induced Altered Expression of Genes Linked to Copper Homeostasis and Subsequent Impact on mSOD1-G85R Aggregation

Another potential hypothesis to explain our observation of USP7 KD affecting mSOD1-G85R aggregation arose from our microarray data, and it pertains to copper homeostasis. Exploration of the microarray data revealed that the copper transporter ATP7A was markedly upregulated in shUSP7 cells compared to controls with a relative

mRNA transcript expression ratio of 2.1886 [36]. This result prompted a literature search aimed at establishing a potential link between expression levels of ATP7A and USP7 and the mSOD1-G85R aggregate phenotype. Copper homeostasis emerged as the underlying theme of the potential pathogenetic model involving all of these proteins.

The relationship between intracellular copper levels and mSOD1-G85R conformation and aggregation has been previously examined. While wild-type (wt) SOD1 is known to bind a copper ion and a zinc ion near its active site, research has shown that binding of a copper ion to an ectopic site of SOD1 plays a key role in maintaining the conformational instability and aggregative nature of monomeric mSOD1-G85R [31, 34]. A 2010 study by Kishigami *et al*. demonstrated via a Cu-IMAC binding column and imidazole elution assay that mSOD1-G85R binds with higher affinity to copper than wt SOD1, and that this mutant protein has increased thiol oxidase pro-oxidant activity which can be toxic to cells [35]. This aforementioned 2010 paper expanded on previous research regarding the sensitivity of the mSOD1-G85R protein to intracellular levels of copper and zinc [31, 35].

Given these previous investigations regarding the effect of copper levels on mSOD1-G85R aggregation in addition to our observed results regarding USP7, the copper transport activity of ATP7A garnered our interest [36]. This protein has previously been linked to neurological pathology, specifically the genetic disorder Menkes disease, which is marked by brain copper deficiency and neurodegeneration [36, 40]. ATP7A is expressed throughout the human body and it normally resides in the trans-Golgi network of cells where it functions in transporting copper to proteins including SOD1 [33, 36, 39]. This protein has been shown to translocate to the plasma

membrane in high intracellular copper conditions where it effluxes the excess metal ions to maintain homeostasis of this potentially toxic specie [33, 36].

The latter activity of ATP7A – functioning to mediate efflux of excess copper from cells – raises an intriguing possibility regarding the cause of our observation of reduced mSOD1-G85R aggregation under the condition of USP7 knockdown. As previously stated, our microarray data demonstrated significant upregulation of ATP7A in USP7 KD cells. It can be hypothesized that this upregulation led to the downstream effect of increased ATP7A-mediated copper efflux from neurons, a feature that ultimately results in a decrease in mSOD1-G85R monomeric aggregate formation given the important role of ectopic copper binding in the generation of this defective protein [32, 34, 35]. Previous research has shown that decreasing intra-neuronal copper levels can have a beneficial impact on the fALS mSOD1 phenotype, and the hypothesis being put forth in this section depends on the validity of these previous findings [35]. Another important issue to consider is the dynamic nature of ATP7A expression and activity. ATP7A functions in both intracellular accumulation of copper, given its roles in the transport of this metal ion across the intestinal mucosa and blood brain barrier, as well as copper efflux from cells in conditions of ion excess [36-37].

There is not a significant amount of previous research regarding the effect of inducing overexpression of ATP7A on copper homeostasis that we could potentially apply to our microarray data. One recent study examined the effect of significant overexpression of ATP7A on the transport of copper across mammary epithelial cells as well as placental tissue in mice [38]. This research group used a transgenic mouse model in which ATP7A was being expressed at a level 10-20x higher than in wild-type mice

[38, 41]. Their observation that ATP7A overexpression led to increased extracellular transport of copper from mammary epithelial cells to pups and across the placenta to developing fetuses may provide support for our proposed model regarding copper efflux from neurons and decreased mSOD1-G85R aggregate formation or stability [38]. It should be noted that the results from this study by Wadwa *et al*. involves significantly higher levels of ATP7A overexpression than what we observed in the USP7 KD cells within our microarray analysis [38].

Going forward, our investigations of this model involving copper homeostasis and the proteins ATP7A, USP7, and mSOD1-G85R aggregation would likely benefit the most by beginning with the examination of ATP7A expression levels closely approximating what we observed in our microarray data. Possible experiments could include co-transfecting mSOD1-G85R cells with an ATP7A overexpression transgene to determine if this copper transport protein has an effect on mSOD1-G85R aggregation independent of altered USP7 activity. Another avenue to explore would be a specific link between USP7 and ATP7A expression given the apparent lack of previous research exploring the relationship between these two proteins. This analysis could be conducted via a binding assay or an examination of the molecular structures of these two proteins in an attempt to uncover possible conformational similarities that would allow them to interact directly.

Hypothesis for USP7 Effect on mSOD1 Aggregation Based on SCA1 Model

An alternative hypothesis that could explain our observed results is based on a study focusing on the disease spinocerebellar ataxia type 1 (SCA1). The authors of this paper suggested that the activity of USP7 in targeting defective ataxin-1 proteins for

proteasomal degradation via polyubiquitin chain regulation is decreased with regards to the mutant form of ataxin-1 [15]. It is possible that there is a similar binding interaction between USP7 and mSOD1, such that the knockdown of USP7 leads to an alteration in the ubiquitination of mSOD1 that causes its increased transport to the UPS and subsequent degradation. As with the previous hypothesis, this idea is simply speculation that is based upon our observations and the background information regarding USP7 that exists within previous literature. Before these possible mechanisms can be explored or elucidated, we must continue to pursue our experiments and more firmly establish a role for this DUB within ALS pathology.

Conclusions

Our investigation into the role of the deubiquitinating enzyme USP7 in fALS pathogenesis has yielded promising results to this point, and the data presented here have illuminated possible avenues to explore for future research into this link. Our primary goal was to more firmly establish the relationship between USP7 knockdown and mSOD1-G85R aggregation that had surfaced through the *C. elegans* siRNA screening experiment [6]. To accomplish this, we performed a rescue experiment in which an exogenous, knockdown resistant (KDR) USP7 genetic construct was co-transfected into mSOD1-G85R-expressing HEK cells along with an shUSP7 construct in an attempt to show a restoration of the aggregate phenotype that has been observed in mSOD1-G85R cells in which USP7 expression is not being altered.

Carrying through with this rescue experiment involved an extensive DNA subcloning process to generate the USP7.KDR gene product as well as an shUSP7 construct. We were able to confirm via restriction enzyme digestions (depicted in Figure 4) as well as DNA sequencing analysis that our genetic constructs had been generated and could be used in the rescue experiment. As shown in the Western blot gel image corresponding to the P2 insoluble fraction samples in Figure 5, we observed partial restoration of the mSOD1-G85R aggregate phenotype in Sample 4 compared with the control samples. While this result was consistent with our initial hypothesis, there are a few mitigating factors that necessitate further investigation to strengthen our result. The lack of complete restoration of the mSOD1-G85R aggregate phenotype in Sample 4 and the unanticipated discrepancy in mSOD1-G85R aggregation in our control samples are issues that were covered in the "Discussion" section. Possible future experiments to

delve more into these issues include retesting the ability of our USP7.KDR construct to restore mSOD1-G85R aggregation in a repeat rescue experiment. Another potential future experiment we discussed involved testing an enzymatically-dead USP7 construct to more closely examine how this gene taxes protein synthesis machinery versus our other control construct containing GFP.

In addition to the DNA subcloning projects and rescue experiment, our investigations of USP7 involved a microarray analysis comparing cells in which this gene was being knocked down to control cells expressing endogenous USP7. The results of this microarray experiment, along with the background literature search that comprises the introductory portion of this paper, brought forth several proteins of interest that could contribute to the pathogenetic mechanism underlying our hypothesized link between USP7 and mSOD1-G85R aggregation. Our future research regarding USP7 should include investigations into whether these proteins involved in cell cycle regulation and in copper homeostasis pathways are involved in mediating the link we have observed between altered USP7 expression and mSOD1-G85R aggregation. We must first work to more firmly establish this proposed link between mSOD1-G85R and USP7, an objective that may ultimately offer further insight into ALS pathogenesis.

Gene	Ratio of expression (USP7 vs. CTRL)	P value for ratio of expression	Gene upregulated or downregulated in shUSP7 sample compared to CTRL
USP7	0.491503	$2.05x10^{-7}$	Downregulated
P53	1.10641	0.00131535	Upregulated
Mdm2	1.47181	$6.75x10^{-5}$	Upregulated
FOXO4	1.21629	$6.81x10^{-5}$	Upregulated
CDKN1A	1.58212	$1.78x10^{-5}$	Upregulated
ATP7A	**2.18826**	**$2.18x10^{-8}$**	**Upregulated**
ATP7B	1.16092	0.00961578	Upregulated
ATOX1	0.911904	0.225093	Downregulated
CCS	0.95171	0.312616	Downregulated
Retinoic acid receptor β	0.891471	0.0967545	Downregulated
COMMD1	**1.11329**	**0.0449607**	**Upregulated**
Clusterin (CLU)	0.82296	0.000897	Downregulated
COX17	1.1376	0.197788	Upregulated

Table 1 Microarray data analysis results for genes linked to USP7/mSOD1-G85R aggregation model focused on cell cycle regulation and copper homeostasis
Ratio of expression is the expression of a gene in cells transfected with an shUSP7 construct versus cells transfected with a control shRNA construct. USP7 is downregulated in shUSP7 versus the control as expected.

Table 1 includes microarray data for a selection of genes including and related to USP7. The "Ratio of expression" column shows a comparison of specific gene-associated mRNA transcript levels in cells transfected with an shUSP7 construct versus cells transfected with a control shRNA construct. The values in this column are contextualized within the column in the far right which explicitly states whether each gene is comparatively upregulated or downregulated in the shUSP7-expressing cells. The downregulation of USP7 expression in the shUSP7 cells was an expected result and could be considered a control for this experiment.

Several of the genes included in this table have been related to USP7 in previous research, and they underlie a model for the observed effect of USP7 knockdown on mSOD1-G85R aggregation that is discussed within this paper. It is noteworthy that p53, FOXO4, and CDKN1A (or p21) mRNA transcript levels were comparatively upregulated in the shUSP7 cells [30]. These observations are consistent with previous results that relate all of these proteins via biochemical pathways. Furthermore, it could be argued that these results support the proposed model of USP7-mediated cell cycle alteration having an impact on mSOD1-G85R aggregation. The observed upregulation of Mdm2 in this microarray analysis does not seem to be consistent with our expected observation based on previous literature. This discrepancy with our other microarray results, particularly given the inclusion of Mdm2, p53, and USP7 within the same pathway, may be explained by regulatory feedback mechanisms that control the expression of these proteins at various levels [11, 13].

The set of genes beginning from ATP7A and moving down in Table 1 were investigated due to the emergence of ATP7A as a potential protein of interest within our

studies of the effects of USP7 knockdown on the mSOD1-G85R aggregate phenotype. Analysis of the microarray data for mRNA transcripts whose expression levels were most significantly impacted in shUSP7 cells revealed marked upregulation of ATP7A in shUSP7 cells. This observed result prompted a literature search that focused on copper homeostasis in the CNS, proteins involved in this process, and the impact of copper levels on mSOD1 aggregation. The proposed model involving these components and their potential relationship to our work with USP7 is covered in the Discussion section.

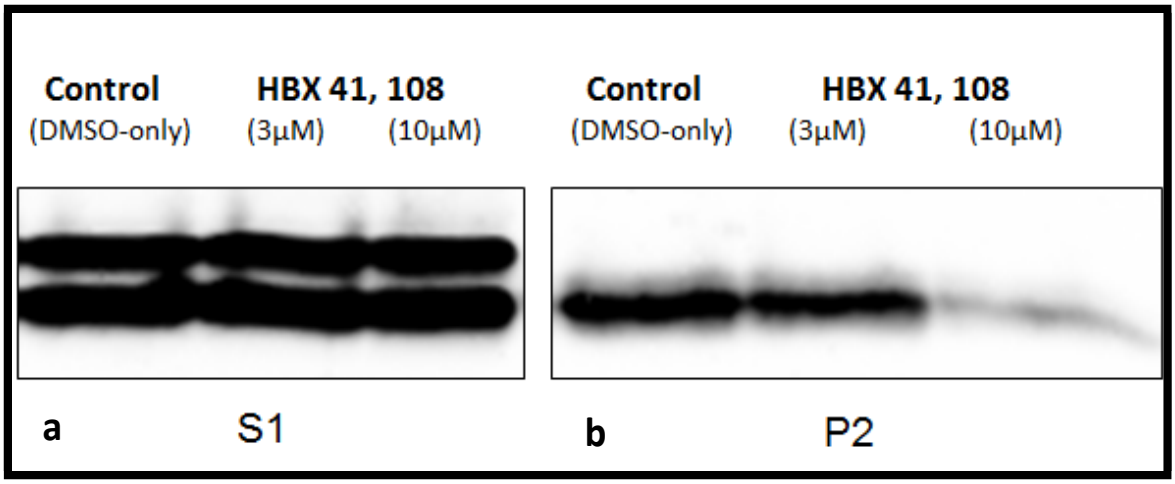

Figure 1 Western blot analysis of mSOD1 expression in cells co-transfected with USP7 inhibitor HBX 41,108. a) Wild type SOD1 protein (top band) and mutant SOD1 protein (lower band) are detected in the control and both HBX41, 108 samples.
b) mSOD1 aggregates are detected in the control and 3 μM HBX41, 108 samples and are reduced in the insoluble (P2) fraction at 10 μM**.**

Figure 1 was obtained from a Western blot assay conducted by Dr. Goran Periz, a postdoctoral researcher in our lab, involving the USP7-inhibiting molecule HBX 41,108. HEK293 cells were transfected with an mSOD1 construct, and the HBX 41,108 was then introduced in certain samples in concentrations of 3 μM and 10 μM so that the effect of USP7 knockdown on mSOD1 aggregation could be studied. This experiment was a follow-up to our lab's previous siRNA worm screen that showed that knockdown of the USP7 gene was associated with a decrease in mSOD1 aggregation.

The membrane on the left depicts the protein bands from the S1 (soluble) fractions for the control DMSO sample as well as two samples containing HBX 41,108 in concentrations of 3 μM and 10 μM. The upper bands in this image correspond to wild type SOD1 protein, and the lower bands correspond to a mutant form of this protein. The membrane on the right depicts the P2 (insoluble) fractions of the same samples as are shown in the S1 image. This membrane is of particular interest as aggregated mSOD1 proteins would be expected to accumulate in the insoluble fractions. It can be seen that the protein bands shown in this image run at the same location (corresponding to protein size) as the mSOD1 bands shown in the S1 image, and thus they correspond to the mSOD1 aggregates. A clear reduction in mSOD1 aggregates appears in the sample containing 10 μM HBX 41,108 compared to the 3 μM HBX 41,108 and DMSO control samples. This observation is consistent with our lab's previous results that linked USP7 knockdown to a decrease in mSOD1 aggregates.

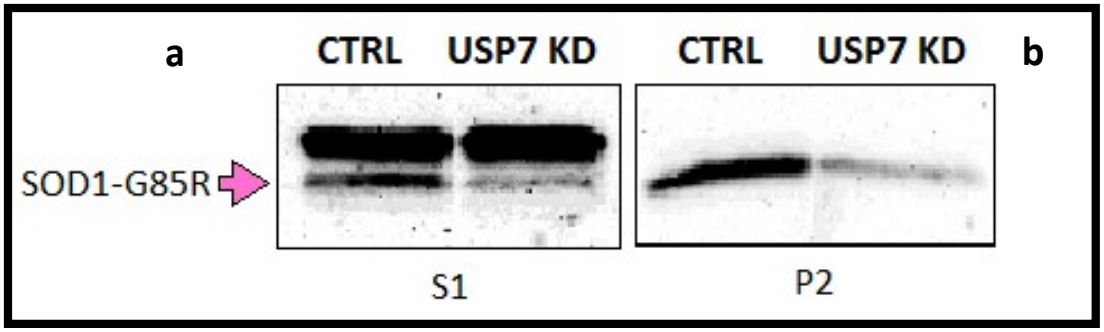

Figure 2 Western blot analysis of mSOD1-G85R aggregate expression cells co-transfected with USP7-specific shRNA construct. a) Comparable levels of wt-SOD1 (top band) are detected in control and USP7 KD samples in the soluble fraction. There is increased expression of mSOD1-G85R (lower band) in the sample corresponding to the cells transfected with control shRNA compared to shUSP7. b) An increased expression of mSOD1-G85R in the sample corresponding to the cells transfected with control shRNA compared to shUSP7 is detected.

Figure 2 depicts the results obtained by Dr. Goran Periz, a postdoctoral researcher in our lab, of a Western blot in which the effect of USP7 knockdown on mSOD1-G85R aggregation was being tested within the HEK cell model. Cells were co-transfected with an mSOD1-G85R construct and either an shRNA control molecule or shUSP7 construct. The membrane on the left side of the image corresponds to the soluble (S1) fractions, and it shows comparable levels of wt-SOD1 expression, indicated by the higher bands, in the control shRNA and shUSP7 samples. The bands corresponding to mSOD1-G85R proteins are indicated by the pink arrow and run below the wt-SOD1 bands. It can be seen clearly from this image that there is increased expression of mSOD1-G85R in the sample corresponding to the cells transfected with control shRNA compared to shUSP7. The apparent decrease in mSOD1-G85R protein accumulation in cells transfected with shUSP7 is also seen in the right membrane, which corresponds to the insoluble (P2) fractions. Once again, the blue arrow indicates the protein bands that correspond to mSOD1-G85R, and there is an apparent increase in insoluble, aggregated proteins in the control shRNA sample compared to the shUSP7 sample. These results are consistent with our lab's previous observation of reduced mSOD1-G85R aggregation within the context of USP7 gene knockdown.

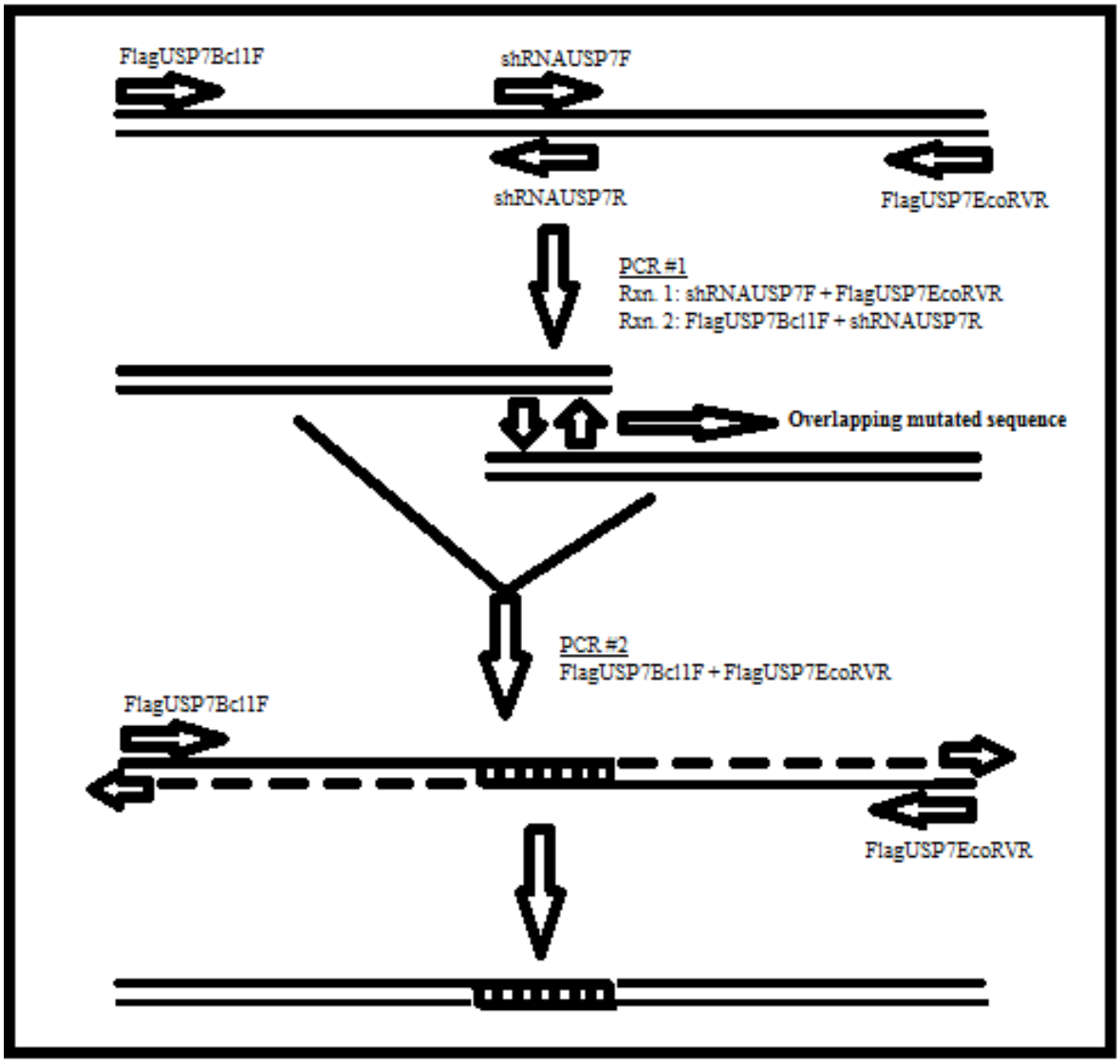

Figure 3 Overlap-extension PCR assay used to generate the knockdown-resistant USP7 construct. Four primers were designed for two PCR steps that ultimately resulted in the formation of a double-stranded construct that included the knockdown-resistant portion of the USP7 gene.

Figure 3 is a diagram of the steps involved in the overlap extension PCR (OE-PCR) assay that was used to generate the knockdown-resistant USP7 genetic construct. This assay is used for site-directed mutagenesis, and in this particular case, our goal was to generate a transgene that would code for USP7 but would not be recognized by our RFP.shUSP7 construct. This process involved four primers that we designed to accomplish this specific goal; the shRNAUSP7F and shRNAUSP7R primers included the mutations in the USP7 sequence that would confer resistance to knockdown by the RFP.shUSP7 construct. As can be seen in the image, the first step of the OE-PCR involved a pair of reactions. The products generated from these two reactions had an overlapping sequence that corresponded to the portion of the USP7 gene in which site-directed mutagenesis had been induced. The next step of this assay involved using the two products generated from PCR #1 as a combined template for a subsequent PCR reaction. The primers used in PCR #2 were FlagUSP7Bcl1F and FlagUSP7EcoRVR, and this reaction led to the formation of our desired double-stranded construct that included the knockdown-resistant portion of the USP7 gene [19, 20]. This fragment was eventually incorporated into a complete USP7 gene so that the effect of rescuing USP7 expression in mSOD1-G85R-expressing cells could be tested.

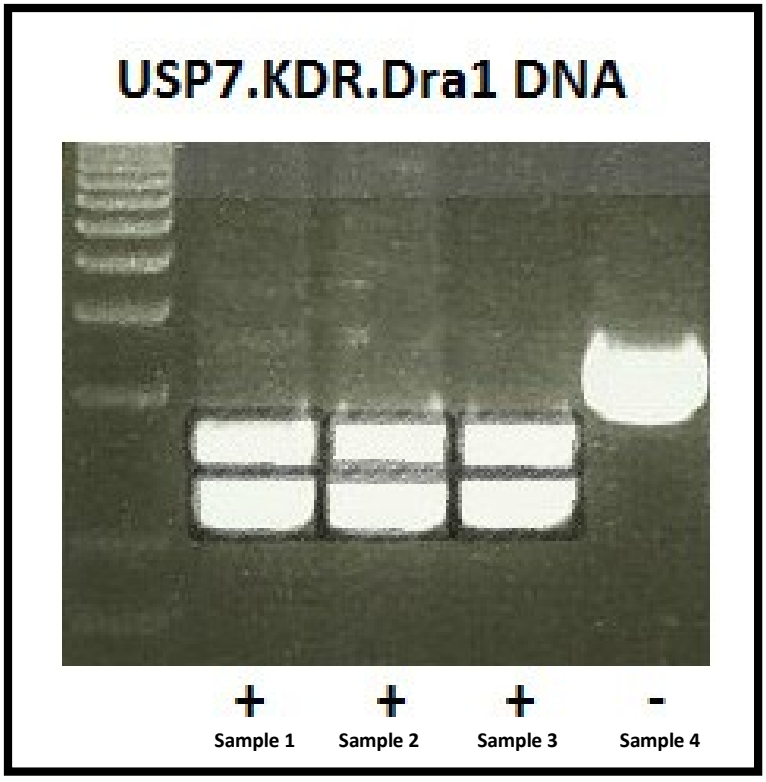

Figure 4 SDS-PAGE image of the Dra1 restriction enzyme digests on the pCI.Flag.HAUSP/USP7.KDR samples. Restriction digests were performed at the end of the subcloning process and expected banding patterns were obtained for Samples 1-3. Sample 4 is a negative clone for the desired pCI/USP7.KDR construct.

Figure 4 corresponds to an assay in which we used restriction digest cuts to test the sequences of our pCI.Flag.HAUSP/USP7.KDR samples that were obtained at the end of the subcloning process. Clones that tested positive based on DNA band size measured against the DNA ladder (labeled by "+" symbols) were subsequently sent for sequencing analysis to confirm that there were not any mutations within our construct. The digestion cuts were performed with the enzyme Dra1, and the expected banding pattern for our construct following these cuts was observed in Samples 1-3 and 5-8. Samples 1-4 are depicted in this figure moving from left to right, with sample 4 representing a negative clone for our desired pCI/USP7.KDR construct.

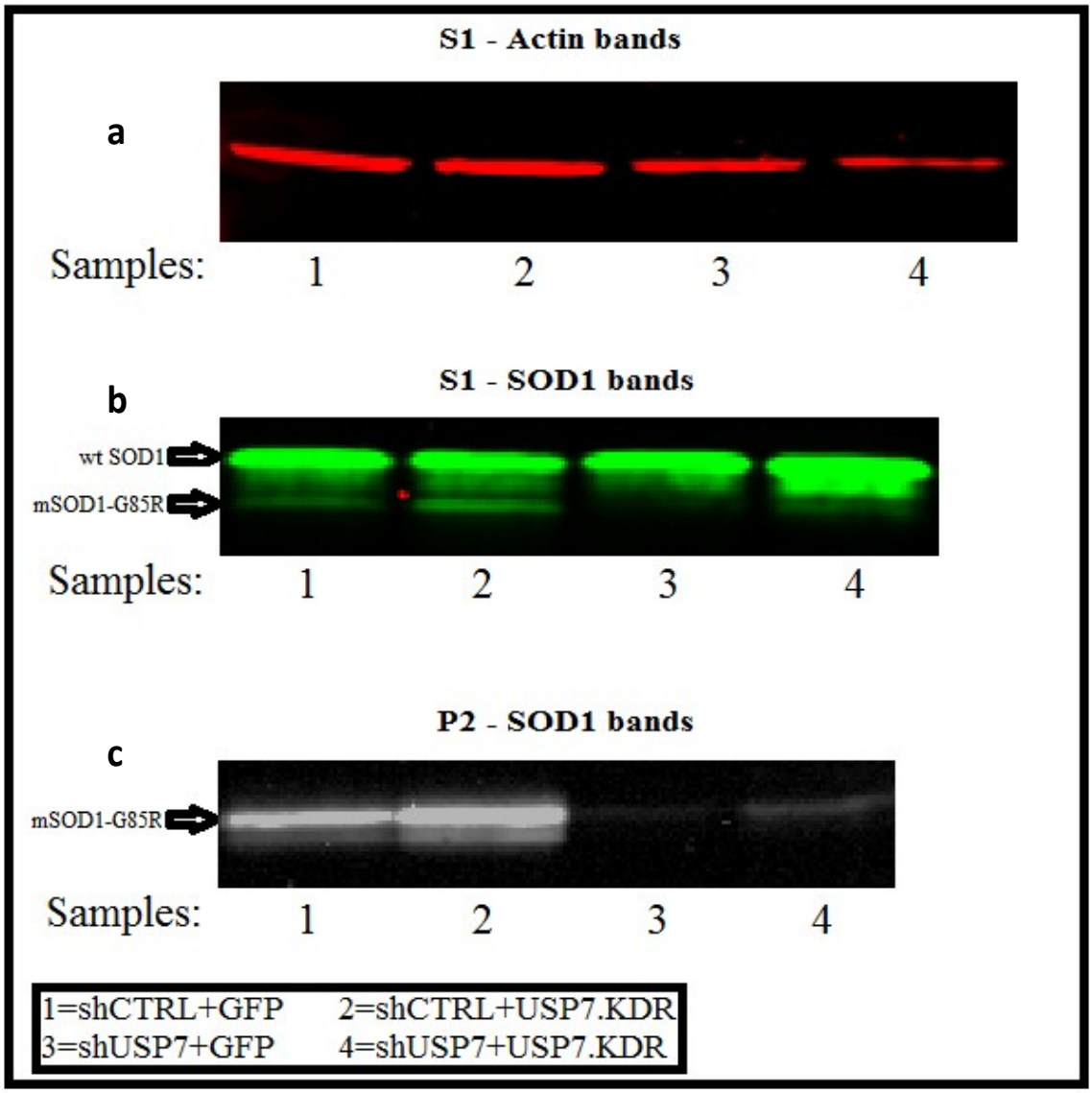

Figure 5 Western blot analysis results for the rescue experiment testing the effects of knockdown-resistant USP7 construct on mSOD1-G85R aggregation a) Actin, the positive control, is detected for Samples 1 to 4, as expected. b) In the soluble fraction (S1), normal SOD1 (top band) and mSOD1-85R (lower band) is shown. c) In the insoluble fraction (P2), a decrease in mSOD1-G85R expression in Sample 3 is detected. Sample 3 included the USP7 shRNA construct, compared to control Samples 1 and 2.

Figure 5 shows the results obtained from the Western blot gels from the USP7.KDR rescue experiment. Part a depicts bands from the S1 samples that correspond to actin, which was stained to serve as an experimental control for protein expression. Part b depicts bands corresponding to SOD1 from the S1 (soluble fraction) samples, with the upper bands representing normal SOD1 and the lower bands showing mSOD1-G85R proteins. Part c depicts bands corresponding to mSOD1-G85R within the P2 (insoluble fraction) samples. The four samples that are depicted in each of these images included an mSOD1-G85R construct as well as the following plasmids: Sample 1 – RFP.shCTRL+pCI.GFP; Sample 2 – RFP.shCTRL+pCI/USP7.KDR.MIDI2; Sample 3 – RFP.shUSP7.1+pCI.GFP; Sample 4 – RFP.shUSP7.1+pCI/USP7.KDR.MIDI2.

Part c shows a decrease in mSOD1-G85R expression in Sample 3, which included the USP7 shRNA construct, as compared to control Samples 1 and 2. This result was consistent with our previous observations regarding the effect of USP7 knockdown on mSOD1-G85R aggregation. Our primary test for this experiment involved a comparison of mSOD1-G85R expression in Samples 3 and 4. As we had hypothesized, Sample 4, which included the USP7 shRNA construct as well as an exogenous, knockdown-resistant USP7 genetic construct, showed a relative increase in aggregate formation. It should be noted that control Samples 1 and 2 showed different levels mSOD1-G85R expression, an unexpected observation that raises the need for further experiments to investigate and confirm our hypothesis.

References

1. Kiernan, Matthew C.; Vucic, Steve; Cheah, Benjamin C.; Turner, Martin R.; Eisen, Andrew; Hardiman, Orla; Burrell, James R.; Zoing, Margaret C. *Amyotrophic Lateral Sclerosis*. The Lancet, 2011, 377, 9769, 942-955.

2. Kabashi, Edor; Durham, Heather D. *Failure of protein quality control in amyotrophic lateral sclerosis*. BBA-Molecular Basis of Disease, 2006, 1762, 11, 1038-1050.

3. Joyce, Peter I.; Fratta, Pietro; Fisher, Elizabeth M. C.; Acevedo-Arozena, Abraham. *SOD1 and TDP-43 animal models of amyotrophic lateral sclerosis: recent advances in understanding disease toward the development of clinical treatments*. Mammalian Genome, 2011, 22, 7, 420-448.

4. Guédat, Philippe; Colland, Frédéric. *Patented small molecule inhibitors in the ubiquitin proteasome system*. BMC Biochem., 2007, Suppl. 1, S14.

5. Lehman, Norman L. *The ubiquitin proteasome system in neuropathology*. Acta Neuropathol., 2009, 118, 3, 329-347.

6. Wang, Jiou; Farr, George W.; Hall, David H.; Li, Fei; Furtak, Krystyna; Dreier, Lars; Horwich, Arthur L. *An ALS-Linked Mutant SOD1 Produces a Locomotor Defect Associated with Aggregation and Synaptic Dysfunction When Expressed in Neurons of* Caenorhabditis elegans. PLoS Genetics, 2009, 5, 1, e1000350.

7. Van der Horst, Armando; de Vries-Smits, Alida M.M.; Brenkman, Arjan B.; van Triest, Miranda H.; van den Broek, Niels; Colland, Frédéric; Maurice, Madelon M.; Burgering, Boudewijn M.T. *FOXO4 transcriptional activity is regulated by monoubiquitination and USP7/HAUSP*. Nature Cell Biology, 2006, 8, 10, 1064-1073.

8. Wijesekera, Lokesh C.; Leigh, P. Nigel. *Amyotrophic lateral sclerosis*. Orphanet Journal of Rare Diseases, 2009, 4, 3, 1-22.

9. Miller, RG; Mitchell, JD; Moore, DH. *Riluzole for amyotrophic lateral sclerosis (ALS)/motor neuron disease (MND)*. Cochrane Database of Systematic Reviews, 2012, 3. Accessed from: http://www.ncbi.nlm.nih.gov/pubmedhealth/PMH0011047/.

10. Nijman, Sebastian M.B.; Luna-Vargas, Mark P.A.; Velds, Arno; Brummelkamp, Thijn R.; Dirac, Annette M.G.; Sixma, Titia K.; Bernards, René. *A Genomic and Functional Inventory of Deubiquitinating Enzymes*. Cell, 2005, 123, 5, 773-786.

11. Hu, Min; Gu, Lichuan; Li, Muyang; Jeffrey, Philip D.; Gu, Wei; Shi, Yigong. *Structural Basis of Competitive Recognition of p53 and MDM2 by HAUSP/USP7: Implications for the Regulation of the p53-MDM2 Pathway*. PLoS Biology, 2006, 4, 2, e27.

12. *About Rilutek*. Rilutek webpage, Sanofi, 2002-2012. Accessed from: http://www.rilutek.com/about-rilutek.

13. Khoronenkova, Svetlana V.; Dianova, Irina I.; Parsons, Jason L.; Dianov, Grigory L. *USP7/HAUSP stimulates repair of oxidative DNA lesions*. Nucleic Acids Research, 2011, 39, 7, 2604-2609.

14. *USP7 ubiquitin specific peptidase 7 (herpes virus-associated) [Homo sapiens]*. NCBI webpage. Accessed from: http://www.ncbi.nlm.nih.gov/gene/7874#reference-sequences.

15. Hong, Sunghoi; Kim, Sung-Jo; Ka, Sojeong; Choi, Inho; Kang, Seongman. *USP7, a Ubiquitin-Specific Protease, Interacts with Ataxin-1, the SCA1 Gene Product*. Molecular and Cellular Neuroscience, 2002, 20, 2, 298-306.

16. Maertens, Goedele N.; El Messaoudi-Aubert, Selma; Elderkin, Sarah; Hiom, Kevin; Peters, Gordon. *Ubiquitin-specific proteases 7 and 11 modulate Polycomb regulation of the* INK4a *tumour suppressor*. The Embo Journal, 2010, 29, 15, 2553-2565.

17. Lee, Eun-Woo; Lee, Min-Sik; Camus, Suzanne; Ghim, Jaewang; Yang, Mi-Ran; Oh, Wonkyung; Ha, Nam-Chul; Lane, David P.; Song, Jaewhan. *Differential regulation of p53 and p21 by MKRN1 E3 ligase controls cell cycle arrest and apoptosis*. The EMBO Journal, 2009, 28, 14, 2100-2113.

18. Sprague, Brian L.; Pego, Robert L.; Stavreva, Diana A.; McNally, James G. *Analysis of Binding Reactions by Fluorescence Recovery after Photobleaching*. Biophysical Journal, 2004, 86, 6, 3473-3495.

19. Ho, Steffan N.; Hunt, Henry D.; Horton, Robert M.; Pullen, Jeffrey K.; Pease, Larry R. *Site-directed mutagenesis by overlap extension using the polymerase chain reaction*. Gene, 1989, 77, 1, 51-59.

20. Heckman, Karin L.; Pease, Larry R. *Gene splicing and mutagenesis by PCR-driven overlap extension*. Nature Protocols, 2007, 2, 4, 924-932.

21. *It's about time: TOPO® PCR cloning technology*. Invitrogen webpage, 2008. Accessed from: http://www.invitrogen.com/etc/medialib/en/filelibrary/pdf/Brochures.Par.30893.File.dat/B-2D071435-TOPO-Bro-FLR.pdf.

22. *Transfection Reagent FAQs*. Life technologies webpage, 2013. Accessed from: http://www.invitrogen.com/site/us/en/home/Products-and-Services/Applications/Cell-Culture/Transfection/transfection-support/Transfection-Reagent-FAQs.html.

23. *Microarrays: Chipping Away At The Mysteries Of Science And Medicine*. NCBI webpage, 2007. Accessed from: http://www.ncbi.nlm.nih.gov/About/primer/microarrays.html.

24. Lo Coco, D.; Marchese, S.; Pesco, M.C.; La Bella, V.; Piccoli, F.; Lo Coco, A. *Noninvasive positive-pressure ventilation in ALS: predictors of tolerance and survival*. Neurology, 2006, 67, 5, 761-765.

25. Zhang, Tao; Hwang, Ho-Yon; Hao, Haiping; Talbot Jr., Conover; Wang, Jiou. Caenorhabditis elegans *RNA-processing Protein TDP-1 Regulates Protein Homeostasis and Life Span*. The Journal of Biological Chemistry, 2012, 287, 11, 8371-8382.

26. *3' IVT Express Kit*. Affymetrix webpage, 2012. Accessed from: http://www.affymetrix.com/estore/browse/products.jsp?categoryIdClicked=&productId=131415#1_1.

27. Schwertman, Petra; Lagarou, Anna; Dekkers, Dick H. W.; Raams, Anja; van der Hoek, Adriana C.; Laffeber, Charlie; Hoeijmakers, Jan H. J.; Demmers, Jeroen A. A.; Fousteri, Maria; Vermeulen, Wim; Marteijn, Jurgen A. *UV-sensitive syndrome*

protein UVSSA recruits USP7 to regulate transcription-coupled repair. Nature Genetics, 2012, 44, 5, 598-602.

28. Kao, Aimee W.; Eisenhut, Robin J.; Martens, Lauren Herl; Nakamura, Ayumi; Huang, Anne; Bagley, Josh A.; Zhou, Ping; de Luis, Alberto; Neukomm, Lukas J.; Cabello, Juan; Farese Jr., Robert V.; Kenyon, Cynthia. *A neurodegenerative disease mutation that accelerates the clearance of apoptotic cells*. Proceedings of the National Academy of Sciences of the United States of America, 2011, 108, 11, 4441-4446.

29. Kalamvoki, Maria; Gu, Haidong; Roizman, Bernard. *Overexpression of the Ubiquitin-Specific Protease 7Resulting from Transfection or Mutations in the ICP0 Binding Site Accelerates Rather than Depresses Herpes Simplex Virus 1 Gene Expression*. Journal of Virology, 2012, 86, 23, 12,871-12,878.

30. *CDKN1A cyclin-dependent kinase inhibitor 1A (p21, Cip1) [Homo sapiens]*. NCBI webpage. Accessed from: http://www.ncbi.nlm.nih.gov/gene/1026.

31. Cao, Xiaohang; Antonyuk, Svetlana V.; Seetharaman, Sai V.; Whitson, Lisa J.; Taylor, Alexander B.; Holloway, Stephen P.; Strange, Richard W.; Doucette, Peter A.; Valentine, Joan Selverstone; Tiwari, Ashutosh; Hayward, Lawrence J.; Padua, Shelby; Cohlberg, Jeffrey A.; Hasnain, S. Samar; Hart, P. John. *Structures of the G85R Variant of SOD1 in Familial Amyotrophic Lateral Sclerosis*. The Journal of Biological Chemistry, 2008, 283, 23, 16,169-16,177.

32. Kiaei, Mahmoud; Bush, Ashley I.; Morrison, Brett M.; Morrison, John H.; Cherny, Robert A.; Volitakis, Irene; Beal, M. Flint; Gordon, Jon W. *Genetically Decreased Spinal Cord Concentration Prolongs Life in a Transgenic Mouse Model of Amyotrophic Lateral Sclerosis*. The Journal of Neuroscience, 2004, 24, 36, 7945-7950.

33. Kozlowski, Henryk; Janicka-Klos, Anna; Brasun, Justyna; Gaggelli, Elena; Valensin, Daniela; Valensin, Gianni. *Copper, iron, and zinc ions homeostasis and their role in neurodegenerative disorders (metal uptake, transport, distribution and regulation)*. Coordination Chemistry Reviews, 2009, 253, 21-22, 2665-2685.

34. Watanabe, Shohei; Nagano, Seiichi; Duce, James; Kiaei, Mahmoud; Li, Qiao-Xin; Tucker, Stephanie M.; Tiwari, Ashutosh; Brown Jr., Robert H.; Beal, M. Flint; Hayward, Lawrence J.; Culotta, Valeria C.; Yoshihara, Satoshi; Sakoda,

Saburo; Bush, Ashley I. *Increased affinity for copper mediated by cysteine 111 in forms of mutant superoxide dismutase 1 linked to amyotrophic lateral sclerosis*. Free Radical Biology and Medicine, 2007, 42, 10, 1534-1542.

35. Kishigami, Hitoshi; Nagano, Seiichi; Bush, Ashley I.; Sakoda, Saburo. *Monomerized Cu,Zn-superoxide dismutase induces oxidative stress through aberrant Cu binding*. Free Radical Biology and Medicine, 2010, 48, 7, 945-952.

36. Zheng, Wei; Monnot, Andrew D. *Regulation of brain iron and copper homeostasis by brain barrier systems: Implication in neurodegenerative diseases*. Pharmacology and Therapeutics, 2012, 133, 2, 177-188.

37. Vonk, Willianne I. M.; de Bie, Prim; Wichers, Catharina G. K.; van den Berghe, Peter V. E.; van der Plaats, Rozemarijn; Berger, Ruud; Wijmenga, Cisca; Klomp, Leo W. J.; van de Sluis, Bart. *The copper-transporting capacity of ATP7A mutants associated with Menkes disease is amerliorated by COMMD1 as a result of improved protein expression*. Cellular and Molecular Life Sciences, 2012, 69, 1, 149-163.

38. Wadwa, Jarrod; Chu, Yu-Hsiang; Nguyen, Nhu; Henson, Thomas; Figueroa, Alyssa; Llanos, Roxana; Ackland, Margaret Leigh; Michalczyk, Agnes; Fullriede, Hendrik; Brennan, Grant; Mercer, Julian F. B.; Linder, Maria C. *Effects of ATP7A overexpression in mice on copper transport and metabolism in lactation and gestation*. Physiological Reports, 2014, 2, 1, e00195, 1-11.

39. Kaler, Stephen G. *ATP7A-related copper transport diseases – emerging concepts and future trends*. Nature Reviews Neurology, 2011, 7, 1, 15-29.

40. Skjorringe, Tina; Tumer, Zeynep; Moller, Lisbeth Birk. *Splice Site Mutations in the ATP7A Gene*. PLoS ONE, 2011, 6, 4, e18599, 1-7.

41. Llanos, Roxana M.; Michalczyk, Agnes A.; Freestone, David J.; Currie, Scott; Linder, Maria C.; Ackland, M. Leigh; Mercer, Julian F. B. *Copper transport during lactation in transgenic mice expressing the human ATP7A protein*. Biochemical and Biophysical Research Communications, 2008, 372, 4, 613-617.

Scholarly Life

Author Darius Farzad was born in Trenton, NJ and was raised in nearby Princeton before matriculating to Johns Hopkins University in September, 2005. After completing his undergraduate studies and obtaining a Bachelor of Arts degree in Public Health, he began the ScM degree program in the Biochemistry and Molecular Biology department at the Johns Hopkins Bloomberg School of Public Health. From there he matriculated to the Drexel University College of Medicine in Philadelphia, PA in August of 2011. He is currently on track to graduate from Drexel with an MD degree in May of 2015, after which he intends to begin residency training in the field of Internal Medicine.